Bioorg. Med. Chem. 37 (2021) 116112

Contents lists available at ScienceDirect

Bioorganic & Medicinal Chemistry

journal homepage: www.elsevier.com/locate/bmc

Identification of two novel thiophene analogues as inducers of autophagy mediated cell death in breast cancer cells

Chandrima Gain [a,1], Aparna Sarkar [b,1], Shrea Bural [a,1], Moumita Rakshit [b], Jeet Banerjee [b], Ankita Dey [b], Nabendu Biswas [c], Gandhi K. Kar [b,*], Abhik Saha [a,*]

[a] School of Biotechnology, Presidency University, Second Campus, Plot No. DG/02/02, Premises No. 14-0358, Action Area-ID, New Town, Kolkata 700156, West Bengal, India
[b] Department of Chemistry, Presidency University, 86/1 College Street, Kolkata 700073, West Bengal, India
[c] Department of Life Sciences, Presidency University, 86/1 College Street, Kolkata 700073, West Bengal, India

ARTICLE INFO

Keywords:
Breast cancer
Tanshinones
Thiophene analogues
Autophagy

ABSTRACT

Natural compounds isolated from different medicinal plants remain one of the major resources of anticancer drugs due to their enormous chemical diversity. Studies suggested therapeutic potential for various tanshinones, key bioactive lipophilic compounds from the root extracts of *Salvia miltiorrhiza* Bunge, against multiple cancers including breast carcinoma. We designed, synthesized and evaluated anti-cancer properties of a series of condensed and doubly condensed furophenanthraquinones of tanshinone derivatives on two breast cancer lines - MCF7 and MDA-MB-231. We identified two thiophene analogues - compounds **48** and **52** with greater anti-proliferative efficiency (~4 fold) as compared to the natural tanshinones. Mechanistically, we showed that both compounds induced autophagy mediated cell death and partial but significant restoration of cell death in the presence of autophagy inhibitor further supported this notion. Both compounds transcriptionally activated several autophagy genes responsible for autophagosome formation along with two death regulators – GADD34

Abbreviations: Tan-I, tanshinone-I; Tan-IIA, tanshinone-IIA; NMR, nuclear magnetic resonance; FT-IR, Fourier-transform infrared spectroscopy; TFA, CF_3CO_2H, trifluoroacetic acid; TFAA, $(CF_3CO)_2O$, trifluoroacetic anhydride; $Pd(PPh_3)_4$, tetrakis(triphenylphosphine)palladium(0); Et_3N, triethylamine; DMF, dimethylformamide; hrs, hours; $NaBH_4$, sodium borohydride; EtOH, ethanol; r.t., room temperature; MsCl, methanesulfonyl chloride; LiCl, lithium chloride; KCN, potassium cyanide; Aq., aqueous; KOH, potassium hydroxide; Na_2HPO_4-H_2O, sodium phosphate dibasic; MeOH, methanol; PBr3, phosphorus tribromide; CHCl3, chloroform; atm., atmosphere; DDQ, 2,3-dichloro-5,6-dicyano-1,4-benzoquinone; HRMS, high-resolution mass spectrometry; ESI, electrospray ionization; LC/MS, liquid chromatography–mass spectrometry; MTT, (3-(4, 5-dimethylthiazolyl-2)-2, 5-diphenyltetrazolium bromide); ER, estrogen receptor; PR, progesterone receptor; Her2, human epidermal growth factor receptor 2; DMSO, dimethyl sulfoxide; μM, micromolar; NADPH, nicotinamide adenine dinucleotide phosphate; nm, nanometer; IC_{50}, the concentration that gives half-maximal response; EtBr, ethidium bromide; AO, acridine orange; DNA, deoxyribonucleic acid; PI, propidium iodide; PARP1, poly [ADP-ribose] polymerase 1; Ex, excitation; Em, emission; GAPDH, glyceraldehyde 3-phosphate dehydrogenase; Bcl-2, B-cell lymphoma 2; Bcl-xL, B-cell lymphoma-extra large; BCL2L1, BCL2 like 1; Bim, Bcl-2 interacting mediator of cell death; BCL2L11, BCL2 like 11; Beclin 1, Coiled-Coil, Moesin-Like BCL2-Interacting Protein; Bax, BCL2-associated X, apoptosis regulator; Bak, BCL2-antagonist/killer 1; LC3, microtubule associated protein 1 light chain 3 alpha/beta; p62/SQSTM1, sequestosome 1; ATG, autophagy related gene; PCR, polymerase chain reaction; RNA, ribonucleic acid; ATG16L1, autophagy related 16 like 1; ATG16L2, autophagy related 16 like 2; GABARAP, GABA (Gamma aminobutyric acid) type A receptor-associated protein; GABARAPL1, GABA type A receptor-associated protein like 1; GABARAPL2, GABA type A receptor-associated protein like 2; PIK3CG, phosphatidylinositol-4,5-bisphosphate 3-kinase catalytic subunit gamma; UVRAG, UV radiation resistance associated gene; DDIT3, DNA damage inducible transcript 3; CHOP, C/EBP (CCAAT/enhancer-binding protein)-homologous protein; GADD34, growth arrest and DNA-damage-inducible protein 34; PPP1R15A, protein phosphatase 1 regulatory subunit 15A; PERK, protein kinase R (PKR)-like endoplasmic reticulum kinase; EIF2AK3, eukaryotic translation initiation factor 2 alpha kinase 3; ATF6, activating transcription factor 6; IRE1, inositol-requiring enzyme 1; ERN1, endoplasmic reticulum to nucleus signaling 1; eIF2α, eukaryotic translation initiation factor 2 alpha; ATF4, activating transcription factor 4; cDNA, complementary DNA; ACTB, actin beta; B2M, beta-2-microglobulin; HPRT1, hypoxanthine phosphoribosyltransferase 1; RPLP0, ribosomal protein lateral stalk subunit P0; CQ, choroquine; GFP, green fluorescence protein; mCherry, mFruits family of monomeric red fluorescent proteins (mRFPs); DCM, dichloromethane; Et2O, diethyl ether; P.E, petroleum ether; EtOAc, ethyl acetate; TLC, thin-layer chromatography; H_2SO_4, sulfuric acid; KBr, potassium bromide; $NaHCO_3$, sodium bicarbonate; Na_2SO_4, sodium sulfate; M.P, melting point; QTOF, Quad Time Of Flight; HCl, hydrochloric acid; FITC, fluorescein isothiocyanate.

* Corresponding authors.
E-mail addresses: gandhi.chem@presiuniv.ac.in (G.K. Kar), abhik.dbs@presiuniv.ac.in (A. Saha).
[1] Equal Contribution.

https://doi.org/10.1016/j.bmc.2021.116112
Received 14 January 2021; Received in revised form 2 March 2021; Accepted 5 March 2021
Available online 17 March 2021

and CHOP for inducing cell death. Altogether, our studies provide strong evidence to support compounds **48** and **52** as promising leads for further development as anticancer agents through modulating autophagy mechanism.

1. Introduction

Salvia miltiorrhiza Bunge (Danshen) has been widely used in traditional Chinese medicine to treat a number of ailments particularly cardiovascular diseases for centuries.[1,2] Subsequently, modern pharmacological studies identified several bioactive molecules - the hydrophilic phenolic acids and the lipophilic tanshinones from dry roots of Danshen exhibiting pro-cardiovascular effects such as expanding the coronary artery and increasing blood flow in the coronary artery, along with anti-oxidant, anti-inflammation, liver protection, immune regulation as well as anticancer properties.[2–4]

The lipophilic components, a large number of condensed furophenanthraquinones and their di-, tetra- and hexahydro derivatives (tanshinones) including tanshinone-I (Tan-I, **1**), tanshinone-IIA (Tan-IIA, **2**), tanshinone-IIB (**3**), tanshindiol-B (**4**), tanshindiol-C (**5**), cryptotanshinone (**6**), nortanshinone (**7**), dihydrotanshinone-I (**8**), isotanshinone-II (**9**) and dihydroisotanshinone-II (**10**) among others with the core nucleus, phenathro[1,2-*b*]furan-10,11-dione and phenathro[4,3-*b*]furan-4,5-dione, have been isolated from dried roots of different Salvia species[5,6] (Fig. 1).

Structurally, all the isolated furophenanthraquinones contains a tetracyclic framework either in "S" shaped form (phenanthro[1,2-*b*] furan-10,11-dione derivatives and its di-, tetra- or *hexa*-hydro derivatives) or in "U" shaped form (phenanthro[4,3-*b*]furan-4,5-dione derivatives or its dihydro derivatives) (Figs. 2 **and S1**).

Among these, particularly Tan-IIA (**2**) and to a lesser extent Tan-I (**1**) have been extensively investigated and reported to exert diverse biological properties. A growing body of evidence indicated potent anticancer properties of tanshinone derivatives against multiple cancers such as cervical cancer, colorectal cancer, gastric cancer, oesophageal cancer, hepatocellular carcinoma, lung cancer, oral cancer, ovarian cancer, osteosarcoma, prostate cancer, and breast carcinoma both in vitro and *in vivo*.[7–18] Despite the potential, further clinical development of tanshinone molecules as anti-cancer agents has been decelerated largely due to its weak potency and exceptionally low aqueous solubility.[19,20] As a result, a number of research groups are currently being engaged on structural optimization to enhance both the anti-cancer potency and the drug-like properties of tanshinone molecules.

In an aim to identify more potent tanshinone analogues, we designed and synthesized eight compounds – **15**, **23**, **25**, **27**, **36**, **43**, **48** and **52** and tested their anti-proliferative activities in two breast cancer lines MCF7 and MDA-MD-231. Recently, thiophene, a sulphur containing heterocyclic scaffold, has emerged as an attractive option for synthesis of library of small molecules exhibiting diverse biological activities including – anti-oxidant, anti-inflammatory, anti-microbial as well as anti-cancer properties.[21,22] Herein, we identified two novel thiophene analogues – compounds **48** and **52** exhibiting increased anti-tumour potency as compared to the natural tanshinones both Tan-I (**1**) and Tan-IIA (**2**). Our results evidently demonstrated that both compounds **48** and **52** induced autophagy mediated cell death in two breast cancer cell lines.

2. Results and discussion

2.1. Synthesis and characterization

Owing to the increasing biological importance of condensed furophenanthraquinones within tanshinone molecules, both synthetic chemists and biologists expressed increased attention in synthesis of a variety of tanshinone derivatives and subsequent exploration of their biological activities particularly as anti-cancer agents.[5,11,20] Likewise, in order to synthesize novel furophenanthroquinones and their analogues, we developed a novel route for synthesis of phenathro[1,2-*b*]furan-10,11-dione and phenathro[4,3-*b*]furan-4,5-dione starting from suitable 1/2-(2-furyl)-3,4-dihydronaphthalen-2-carbaldehyde derivatives as reported earlier.[23,24] The method has great potential in synthesis of both "S" and "U" shaped tetracyclic furophenanthroquinones as well as tricyclic furonaphthoquinones with various substituents in ABCD (or BCD rings in case of furonaphthoquinone) rings of the core nucleus.[23,24] Herein, we synthesised phenanthro[2,1-*b*]furan-10,11-dione (**15**), as nuclear analogue of tanshinones following similar strategy. To this end, we used (2-Bromo-naphthalen-1-yl)-acetic acid methyl ester (**11**) and 3-furanboronic acid as starting material (Scheme 1).

The compound **11** was subjected to Pd (0) catalyzed Suzuki Coupling

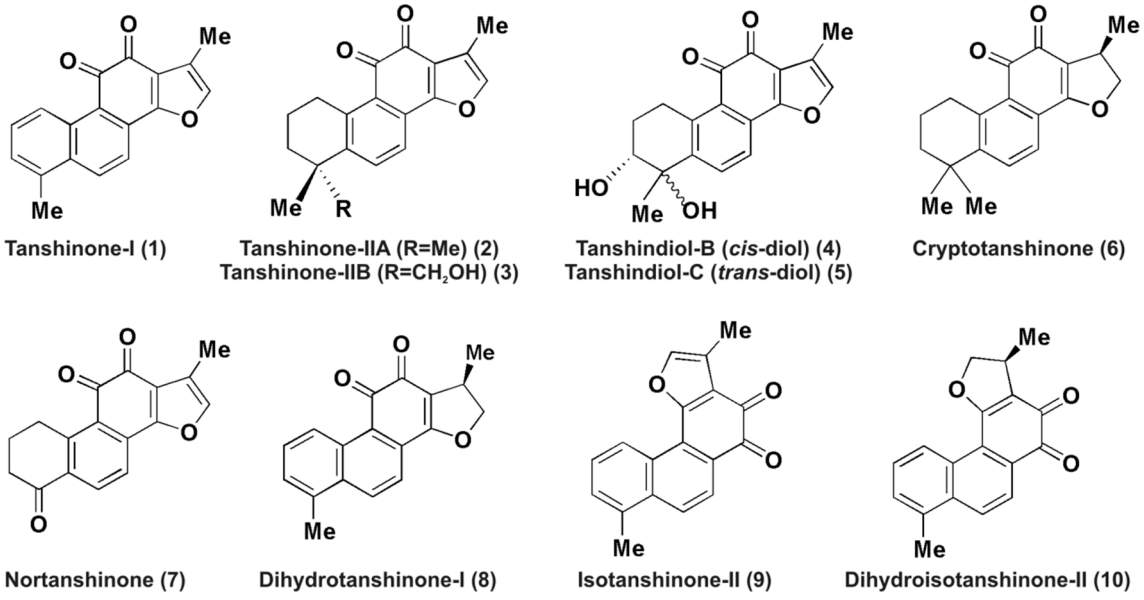

Fig. 1. Various tetracyclic furophenanthraquinone derivatives isolated from dry root extracts of *different Salvia* species.

Reaction with 3-furanboronic acid to furnish [2-(furan-3-yl)-naphthalen-1-yl] acetic acid methyl ester (**12**) as a colourless solid in 70% yield. In IR spectra, the compound showed a strong absorption at 1750 cm^{-1} characteristics of the ester carbonyl group. ^{1}H NMR of the compound **12** was also in agreement with the assigned structure. Alkaline hydrolysis of the ester **12** afforded the corresponding acid **13** in 74% yield. The corresponding FT-IR spectroscopic analysis also demonstrated a strong absorption at 1690 cm^{-1} for COOH group. The carboxylic acid **13** was then cyclised in the presence of TFA/TFAA to furnish the phenol **14** in 77% yield. ^{1}H NMR spectra confirmed the assigned structure of the phenol **14**. At the final step of the synthesis, the target quinone molecule **15** was achieved as a dark red solid in 56% yield, by Fremy's salt oxidation of phenol **14**. The quinone **15** was characterized by usual spectroscopic data (^{1}H NMR, ^{13}C NMR, FT-IR and Mass spectroscopy).

Another novel 'U' shaped furophenanthraquinone i.e. phenanthro [3,4-*b*]furan-4,5-dione (the core nucleus of isotanshinone II) was synthesized starting from 1-bromo-2-naphthaldehydes (**17**) and 3-furanboronic acid (Scheme 2). The two key steps involve in this methodology were i) Suzuki coupling of an aryl halide and furanboronic acid to form aryl-furyl bond and ii) development of *o*-quinone functionality by oxidation of a phenolic moiety (Fig. 3).

The compound **18** was synthesized by the Suzuki coupling of 1-bromo-2- naphthaldehyde (**17**) with 3-furanboronic acid using Pd $(PPh_3)_4$ as the catalyst, Et_3N as the base and DMF as the solvent at 100 °C under Argon atmosphere (Scheme 2). The aldehyde **17** was efficiently prepared from 1-tetralone using modified Vilsmeier-Haack reaction, followed by aromatisation, as reported earlier.[23] After confirming the structure by spectroscopic analysis, the furyl naphthaldehyde (**18**) was then reduced with $NaBH_4$ to the alcohol **19,** which on treatment with mesyl chloride, lithium chloride in the presence of *s*-collidine, furnished the corresponding chloromethyl derivative, which without further purification was directly subjected to reaction with KCN in DMF to obtain the corresponding cyanomethyl derivative **20**. The nitrile **20** on hydrolysis (KOH, EtOH-H_2O) afforded the carboxylic acid **21** as a light brown solid and was then cyclised to the corresponding furophenanthrenol **22** in excellent yield on treatment with a mixture of TFA and TFAA at 0 °C. The phenol **22** was then oxidized by Fremy's salt to the target *o*-quinone **23** as a brick red solid in 77% yield.

Next, we intended to modify the D ring of the isotanshinone-II core nucleus by replacing the furan ring with a thiophene ring. To this end, we utilized thiophene boronic acid instead of furan boronic acid for the aryl-thienyl bond formation by Suzuki reaction. The synthesis of phenanthro[4,3-*b*]thiophene-4,5-dione[5] (**25**) as the thiophene analogue of the ABCD ring system of isotanshinone-II was achieved using the same reaction sequence, which was previously employed in the synthesis of "U" shaped furophananthraquinones starting from 3,4-Dihydro 1-(2-thienyl)naphthalene-2-carbaldehyde[25] (**24**) and 2-thiophene boronic acid (Scheme 3).[5] All the compounds were subsequently characterized by standard spectroscopic evaluation (vide experimental).

As depicted in Scheme 4, synthesis of a regioisomeric 'U'-shaped novel thienophenanthraquinone, 10-methoxyphenanthro[3,4-*b*]thiophene-4,5-dione (**27**) commenced from 3,4-dihydro-1(3-thienyl)-7-methoxynaphthalene-2-carbaldehyde[25] (**26**) as starting material by following the similar protocol as reported earlier[5] with good to very good yields.

Next, modifications were introduced in both rings A and D of the core nucleus present in the naturally occurring furophenanthraquinone, isotanshinone-II molecule. It is well known that bioisosteric relationship exists between benzene and thiophene ring where 'CH = CH' is considered as equivalent to 'S'. So the synthesis of bisthiophene condensed naphthoquinones, *viz.* 9-methylnaphtho[1,2-*b*:7,8-*b*′]bisthiophene-4,5-dione (**36**) and 9-methylnaphtho[2,1-*b*:7,8-*b*′]bisthiophene-4,5-dione (**43**) were achieved where ring A of phenanthro[4,3-*b*] furan-4,5-dione (the core nucleus of isotanshinone II) was replaced by a 2-methylthiophene moiety while ring D was modified with a thiophene moiety (Fig. 4).

Several reports suggested that thiophene analogues represent a rich source of potential scaffolds in search of novel bioactive compounds as anti-micriobial, anti-inflammatory as well as anti-cancer agents.[26,27] It would be worthwhile to explore the possibility in generating new compounds by fusing differently substituted moieties which may offer enhanced pharmacological activities. Therefore, to explore many more systematic modifications on thiophene moiety warrants further investigation. As described in Fig. 4, the thiophene analogue compound **36** may be considered as Bioisostere of thienophenanthraquinone and compound **43** is the nuclear analogue of 'U'-shaped thienophrenanthraquinone. The target molecules **36** and **43** were synthesised from a common precursor 4-bromo-6,7-dihydro-2-methylbenzo[*b*]thiophene-5-carbaldehyde (**29**) (which was obtained from 6,7-dihydro-2-methylbenzo[*b*]thiophen-4(5*H*)-one[28] (**28**) *via* Vilsmeier-Haack reaction) and two different aryl boronic acids, 2-thiopheneboronic acid and 3- thiopheneboronic acid, respectively instead of 2/3-furanboronic acids following Scheme 5 and Scheme 6.

The target compound **36** was synthesized starting from 4-bromo-6,7-dihydro-2-methylbenzo[*b*]thiophene-5-carbaldehyde (**29**) and 2-thiophene boronic acid (Scheme 5). Bromoaldehyde **29** was obtained from the ketone **28** in 73% yield on reaction with PBr_3/DMF in $CHCl_3$. Suzuki coupling of compound **29** with 2-thiopheneboronic acid followed by aromatization (DDQ, benzene, reflux) of the resulting product **30** furnished compound **31** in very good yields. Following the protocol of functional group transformation —CHO → —CH_2OH → —CH_2Cl → —CH_2CN, synthesis of the nitrile derivative **33**, a colourless solid was achieved in very good to excellent yields in all steps. Alkaline hydrolysis (KOH, EtOH-H_2O, reflux) of the nitrile derivative produced the carboxylic acid **34** in 50% yield. The carboxylic acid (**34**) was then cyclised (TFAA-TFA, 0 °C) to 9-methylnaphtho[1,2-*b*:7,8-*b*′]bisthiophen-4-ol (**35**) in excellent yield. Finally oxidation of compound **35** with Fremy's salt produced the target compound 9-methylnaphtho[1,2-*b*:7,8-*b*′]bisthiophene-4,5-dione (**36**) as a deep violet solid in 77% yield. Following a

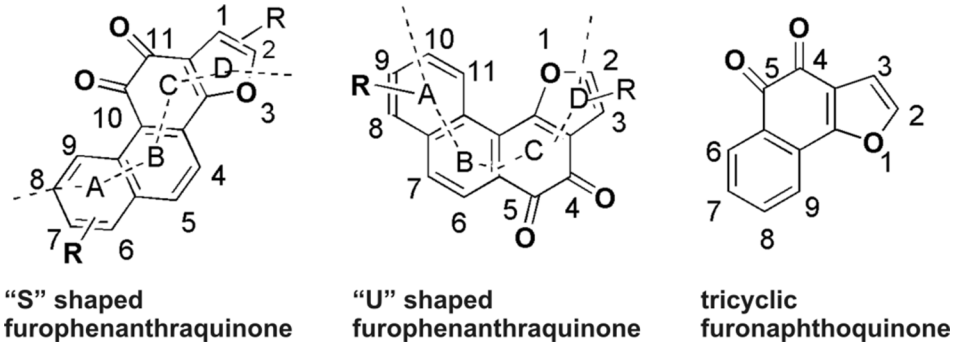

Fig. 2. Core nucleus of "S", "U" shaped furophenanthraquinone and furonaphthoquinone.

similar sequence of reactions, synthesis of the regioisomeric compound 9-methylnaphtho[2,1-*b*:7,8-*b*′]bisthiophene-4,5-dione (**43**) was achieved in eight steps, starting from the bromoalfdehyde **29** and 3-thiopheneboronic acid (Scheme 6).

Anticancer activities of various naphthoquinone derivatives condensed with heterocyclic moiety such as furan, dihydrofuran, thiophene, pyran among others have been widely reported and many distinct mechanisms of action have been attributed to them.[29,30] Importantly, cyclic ether-fused tricyclic naphthoquinones are major pharmacophores due to their significant antibacterial as well as anticancer properties.[30] However, tricyclic naphthoquinones have not yet been reported from natural sources. Nevertheless, a number of reports indicated the synthesis of this class of theino/furonaphthoquinones.[31–34] Notably, a number of naphthoquinones including naphtho[2,1-*b*]thiophene-4,5-diones, naphtho[1,2-*b*]thiophene-4,5-diones and naphtho[2,3-*b*]thiophene-4,9-diones demonstrated potential anticancer activities.[35,36] We have developed a synthetic route for the furonaphthoquinones as described earlier.[24]

Next, we projected to synthesis two more thienonaphthoquinone derivatives as a extension of our methodology starting from commercially available methyl(2-bromophenyl)-acetate (**44**) and thiopheneboronic acids and subsequently achieved compounds **48** and **52** *via* a novel and considerably short synthetic route (Scheme 7 and Scheme 8). As depicted in Scheme 7, the naphthoquinone **48**, as a thiophene analogue, simulates BCD rings of isotanshinone-II core nucleus. Pd(0)-catalysed Suzuki coupling of the ester **44** with 2-thiopheneboronic acid produced methyl 2-[2-(2-thienyl)phenyl]acetate (**45**) as a pale yellow oil in good yield. In IR spectrum, it showed strong absorption at 1738 cm^{-1} for the —CO_2CH_3 functionality. ^1H NMR, ^{13}C NMR and HRMS data also justified the assigned structure (vide experimental). Subsequent hydrolysis of **45** to the carboxylic acid **46**, followed by cyclisation to naphtho[1,2-*b*]thiophen-4-ol (**47**) was achieved in excellent yield. The carboxylic acid **46** exhibited a strong absorption band around 1693 cm^{-1} for the presence of —CO_2H group. ^1H NMR, ^{13}C NMR and HRMS analysis also justified the assigned structure of the compound **47**.

Oxidation of the intermediate phenol **47** with Fremy's salt furnished the target molecule **48** in very good yield (scheme 8). In IR spectrum, the compound **48** exhibited a broad absorption band around 1659 cm^{-1} for the presence of carbonyl groups. ^1H NMR (400 MHz, $CDCl_3$) spectral data of the compound **48** is in conformity with the assigned structure. ^{13}C NMR [(100 MHz, $CDCl_3$): δ = 124.72, 126.08, 127.80, 129.10, 129.73, 130.28, 132.41, 135.85, 136.55, 151.27, 173.86, 180.47 ppm] as well as HRMS data [(ESI+): *m/z* $[M+H]^+$ calcd for $C_{12}H_7O_2S$: 215.0089; found: 214.9340 and [M+Na] calcd for $C_{12}H_6O_2SNa$: 236.9986; found: 236.9225] also supported the structure.

Following a similar reaction sequence starting from same ester **44** and 3-thiopheneboronic acid, the synthesis of naphtho[2,1-*b*]thiophene-4,5-dione (**52**) was accomplished successfully (Scheme 8).

In sum, we successfully synthesized a total of eight novel phenanthtraquinone derivatives with thiophene and furan moieties as tanshinone analogues including compounds **15**, **23**, **25**, **27**, **36**, **43**, **48** and **52**. The structures of synthesized analogues were confirmed using relevant spectroscopic techniques – FT-IR, ^1H NMR, ^{13}C NMR and HRMS. Fourier-transform infrared (FT-IR) analysis confirmed the presence of the major functional groups on different analogues. The calculated molecular weights of the individual compounds were established by the presence of $[M+1]^+$ or $[M+Na]^+$ molecular ion peaks in HRMS data. 1D NMR analysis confirmed the expected chemical shifts of the different H and C present in each compound.

General screening for in vitro anti-proliferative activities of synthesized compounds: The growth inhibitory effects of all the eight synthesized derivatives of natural tanshinones – compounds **1** (Tan-I) and **2** (Tan-IIA) were initially assessed against two human breast cancer cell lines i.e. MCF-7 and MDA-MB-231 using MTT assays to select the most promising ones for further screenings and mechanistic evaluation. While they have many phenotypic and genotypic variations, both MCF7 and MDA-MB-231 breast cancer cells are invasive in nature. However, as compared to hormone dependent MCF7 cells (estrogen and progesterone receptor positive; ER^+PR^+), MDA-MB-231 cells (triple negative, $ER^-PR^-Her2^-$) represent a more aggressive form breast cancer phenotype.[37,38]

Cells plated in 96 well plate were either left untreated (DMSO control) or treated with various compounds with increasing concentrations (0–40 μM). 24 h post-treatment cells were subjected to MTT assay as described in the Experimental Section to determine the cell viability. MTT (3-(4,5-dimethylthiazol-2-yl)-2,5-diphenyltetrazolium bromide) mediated cell-viability is a colorimetric assay, where the NADPH-dependent oxidoreductase enzymes released from viable cells convert the yellow tetrazolium dye to insoluble purple formazan crystals. The absorbance measured at 540 nm of the purple crystals solubilized in DMSO indicate the percentage of viable cells. Subsequently IC_{50} values were calculated for each compound in both cell lines and are summarized in Table 1. Overall, the results confirmed that furophenanthraquinone could serve as a potential scaffold for new anticancer agents with a cytotoxic activity in the micromolar range. MTT assay revealed that two naphthoquinone derivatives **48** (IC_{50} = 1.94 in MCF7 and 2.59 μM in MDA-MB-231) and **52** (IC_{50} = 1.85 in MCF7 and 2.95 μM in MDA-MB-231), bearing thiophene moieties, induced most significant growth inhibition compared to the rest of the compounds, in both breast cancer lines (Table 1). In both cell lines, these derivatives were found to be around 4-fold more potent than the natural tanshinones – compounds **1** (IC_{50} = 7.92 in MCF7 and 7.96 μM in MDA-MB-231) and **2** (IC_{50} = 7.79 in MCF7 and 7.79 μM in MDA-MB-231). While compound **27**, another thiophene analogue, retained anti-proliferative activity parallel to those of the parent tanshinones (**1**, **2**) in MCF7 and MDA-MB-231, with IC_{50} of 8.02 and 6.00 μM, respectively, the other five compounds **15**, **23**, **25**, **36** and **43** were remarkably less potent (~2–3-fold) compared to the natural tanshinones with IC_{50} range from 12.79 to 23.43 μM in both cell lines.

Compounds 48 and 52 exhibit anti-proliferative activities by inducing cell apoptosis: The two most potent thiophene analogues compounds **48** and **52** along with compound **27** and two naturally occurring tanshinone molecules (**1** and **2**) were selected for further analyses. In order to corroborate compounds **48** and **52** mediated enhanced anti-proliferative activities, alterations of cell morphology were observed in a phase contrast microscope in both MCF7 and MDA-MB-231 lines at different time points (0, 6, 12 and 24 h) at 2.5 μM concentration (**Fig. S53A-B**). Both compounds **48** and **52** treatment caused a drastic difference in cell death percentage in comparison to that

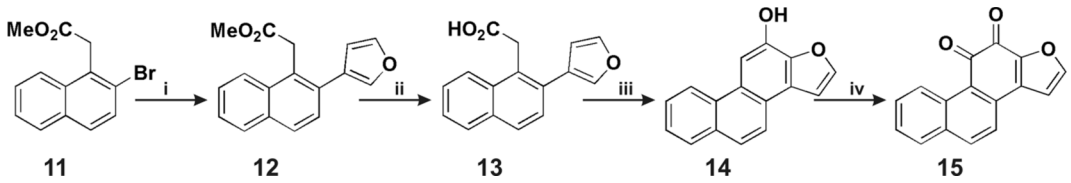

Scheme 1. Synthesis of phenanthro[2,1-*b*]furan-10,11-dione (**15**).
Reagents and conditions: (i) 3-Furanboronic acid, TEA, $Pd(PPh_3)_4$, DMF, 110 °C, 7 h, 70%. (ii) 20% aqueous KOH solution, methanol, reflux, 9 h, 74%. (iii) TFAA, TFA, r.t, 12 h, 75%. (iv) Fremy's salt, 1/6 M aqueous solution of Na_2HPO_4, MeOH, 0 °C to r.t, 12 h, 57%.

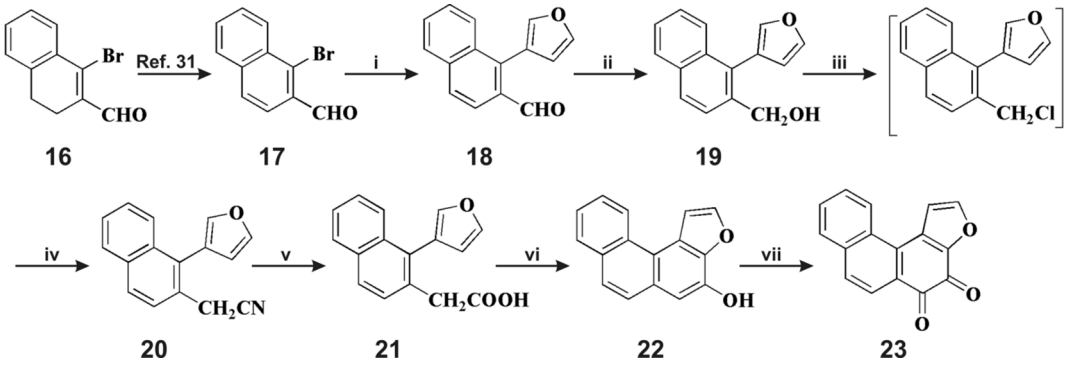

Scheme 2. Synthesis of Phenanthro[3,4-*b*]furan-4,5-dione (**23**).
Reagents and conditions: i) 3-furanboronic acid, $Pd(PPh_3)_4$ (1 mol%), Et_3N, DMF, 100 °C, 10 hrs under Aratm., 61%; ii) $NaBH_4$, EtOH, r.t., 2 hrs, 97%; iii) MsCl, *s*-collidine, LiCl, DMF, 0 °C-r.t., overnight; iv) KCN, DMF, 7 hrs, 76%; v) Aq. KOH, EtOH, reflux, 18 hrs, 82%; vi) TFAA-TFA, 0 °C-r.t., overnight, 83%; vii) Fremy's salt, Na_2HPO_4-H_2O, MeOH, overnight, 77%.

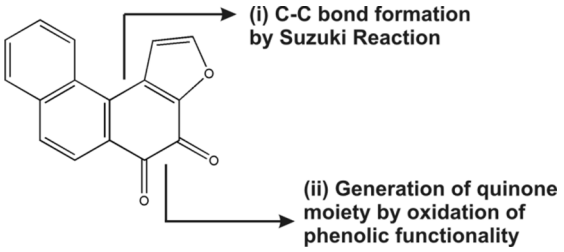

Fig. 3. Synthetic strategy for "U" shaped furophenanthraquinone nucleus.

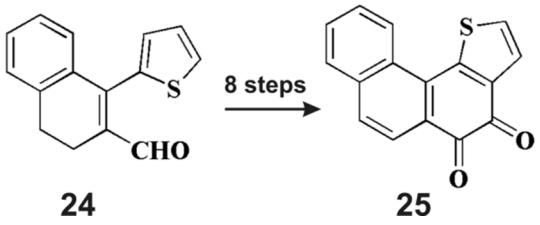

Scheme 3. Synthesis of Phenanthro[4,3-*b*]thiophene-4,5-dione (**25**).

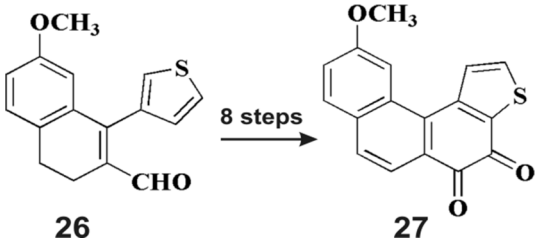

Scheme 4. Synthesis of 10-methoxyphenanthro[3,4-*b*]thiophene-4,5-dione (**27**).

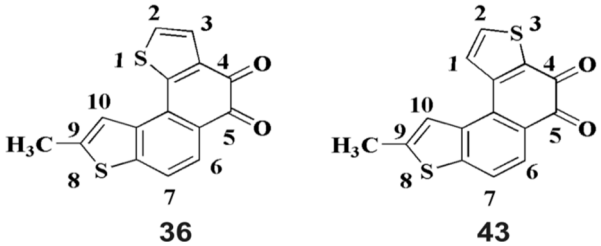

Fig. 4. Bis(heteroannulated)naphthoquinones **36** and **43.**

of natural tanshinones Tan-I (**1**) and Tan-IIA (**2**) (**Fig. S53A-B**). In agreement with the MTT assays, compounds **48** and **52** treatment resulted in significant reduction in cell number and size of both MCF7 and MDA-MB-231 cells in a time dependent manner (**Fig. S53A and S53B, respectively**). In contrast, compound **27** showed similar activity as that of the parent compounds 1 and 2 (**Fig. S53A-B**).

To determine whether the cytotoxic effect of compounds **48** and **52** on breast cancer cells was induced by apoptosis, cells were either left untreated (DMSO control) or treated with 2.5 μM compounds **1**, **2**, **27**, **48** and **52** for 24 h, stained with 1:1 solution of ethidium bromide (EtBr) and acridine orange (AO) and viewed in a fluorescence microscope. While AO stains live cells as green, EtBr stains the DNA as red in case of apoptosis and necrosis. Therefore, apoptotic cell are observed as distinct red nucleus in live green cells, while non-viable or necrotic cells are fully stained red. The representative microscopy images of each panel demonstrated a significant increase of cell death in response to compounds **48** and **52** treatment compared DMSO control and other compounds including **1**, **2** and **27** (**Fig. S53C**). The percentage of apoptotic and necrotic cells were calculated with respect to live cells and plotted as bar diagrams (**Fig. S53D**). As expected, the results demonstrated that compounds **48** and **52** induced cell death ~2-fold more than that of Tan-IIA (**Fig. S53E**). Compound **27** showed similar activity as that of Tan-IIA, while at this concentration Tan-I did not show any cell death (**Fig. S53D**).

To further validate this data, the cell apoptosis assay was performed by Annexin V/PI staining of drug treated cells using a similar experimental setup. The percentage of overall apoptotic cells was determined from the sum of early apoptosis (Annexin V^+/PI^-) and late apoptosis (Annexin V^+/PI^+) in both MCF7 and MDA-MB-231 cell lines (Fig. 5**A and 5B, respectively**). In agreement with the previous results, compounds **48** and **52** exhibited significant stronger effects (>2–20 folds) on apoptotic induction as compared to the natural tanshinones – compounds **1** and **2** along with compound **27** in both cell lines (Fig. 5**A and 5B**). Although compounds **48** and **52** treatment showed comparable total cell death (74.7% and 77.1% in MCF7; 66.3% and 66.4% in MDA-MB-231), compound **52** induced more apoptosis than that of compound **48** (37.0% vs. 54.9% in MCF7; 22.8% vs. 39.6% in MDA-MB-231) (Fig. 5**A and 5B, bar diagrams**). Interestingly, the results indicated that among the two natural tanshinones, compound **1** (Tan-I) distinctively induced apoptosis in MCF7 line (15.21% vs. 1.62%), in contrast compound **2** (Tan-IIA) mediated apoptosis was specific to triple negative breast cancer line (9.57% vs. 3.21%) (Fig. 5**A and 5B, bar diagrams**). Importantly, in addition to cell apoptosis compounds **48** and **52** also demonstrated a significant increase in other types of cell death including necrosis (Fig. 5**A and 5B**). To re-validate compounds **48** and **52** mediated enhanced apoptotic induction, western blot analyses was performed against cleaved PARP1, a hallmark of apoptosis (Fig. 5**A**). As

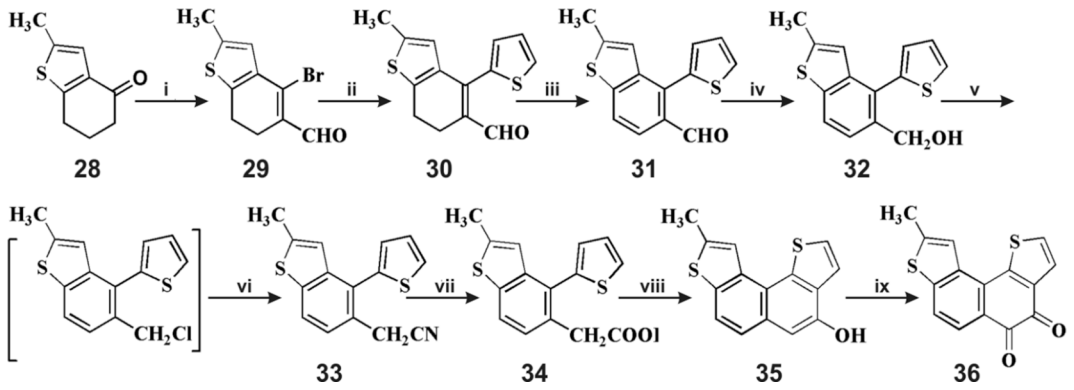

Scheme 5. Synthesis of 9-methylnaphtho[1,2-*b*:7,8-*b*′]bisthiophene-4,5-dione (**36**).
Reagents and Conditions: i) PBr_3, DMF, $CHCl_3$, 0 °C-r. t., 16 hrs, 73%; ii) 2-thiopheneboronic acid, $Pd(PPh_3)_4$, Et_3N, DMF, 110 °C, N_2 atm., 10 hrs, 61%; iii) DDQ, benzene, reflux, 24 hrs, 86%; iv) $NaBH_4$, EtOH, r.t., 2 hrs, 91%; v) MsCl, LiCl, *s*-collidine, DMF, 0 °C overnight; vi) KCN, DMF, 11 hrs, 84%; vii) KOH, EtOH-H_2O reflux, 20 hrs, 50%; viii) TFAA-TFA, 0 °C overnight, 80%; ix) Fremy's salt, 1/6M Na_2HPO_4 buffer solution, MeOH, 0–5 °C, overnight, 77%.

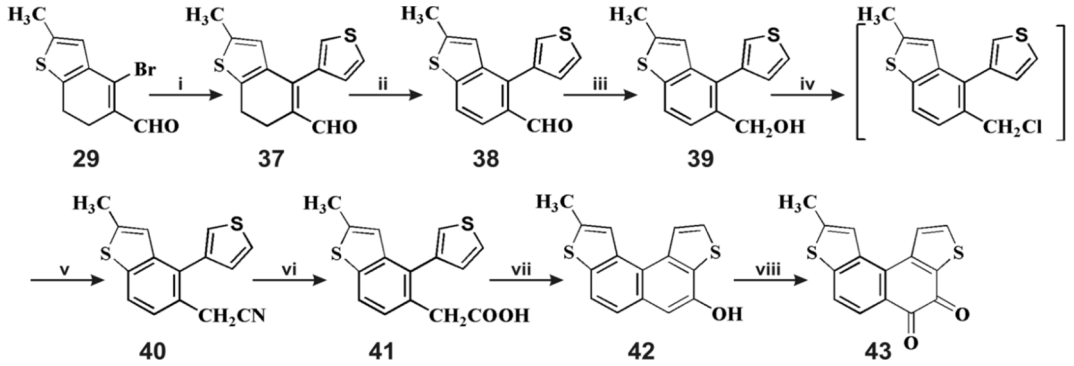

Scheme 6. Synthesis of 9-methylnaphtho[2,1-*b*:7,8-*b*′]bisthiophene-4,5-dione (**43**).
Reagents and Conditions: i) 3-thiopheneboronic acid, $Pd(PPh_3)_4$, Et_3N, DMF, 110 °C, N_2 atm., 10 hrs, 67%; ii) DDQ, benzene, reflux, 24 hrs, 89%; iii) $NaBH_4$, EtOH, r.t., 2 hrs, 94%; iv) MsCl, LiCl, *s*-collidine, DMF, 0 °C overnight; v) KCN, DMF, 11 hrs, 89%; vi) KOH, EtOH-H_2O reflux, 20 hrs, 58%; vii) TFAA-TFA, 0 °C overnight, 93%; viii) Fremy's salt, 1/6M Na_2HPO_4 buffer solution, MeOH, 0–5 °C, overnight, 83%.

similar to Annexin/PI staining, compound **52** and to a lesser extent (~2-fold) compound **48** treatments led to a marked increase of PARP cleavage in both cell lines (Fig. 5**C and 5D**).

Compounds 48 and 52 induce both apoptosis and autophagy: In response to several anticancer therapies, two essential forms of cell death mechanisms often arise concurrently that includes 'programmed cell death type I' or apoptosis and 'programmed cell death type II' or autophagy. While apoptosis is the primary cell death mechanism, autophagic pathway in general plays a cytoprotective role through which cancer cells avoid various deleterious effects caused by

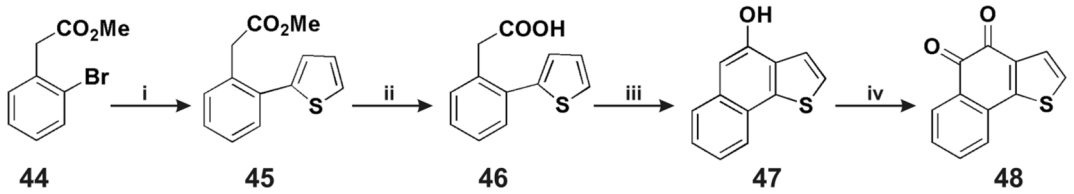

Scheme 7. Synthesis of naphtho[1,2-*b*]thiophene-4,5-dione.
Reagents and conditions: (i) 2-thiopheneboronic acid, Et_3N, DMF, $Pd(PPh_3)_4$, 110 °C, N_2 atm., 6 hrs, 65%; (ii) KOH, EtOH, H_2O, reflux, 12 hrs, 78%; (iii) TFAA-TFA, 0 °C, overnight, 80%; (iv) Fremy's salt, 1/6 M aq. Na_2HPO_4, MeOH, r.t., overnight, 72%.

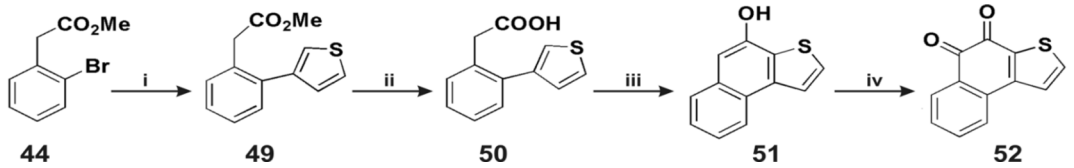

Scheme 8. Synthesis of naphtho[2,1-*b*]thiophene-4,5-dione.
Reagents and conditions: (i) 3-thiopheneboronic acid, Et_3N, DMF, $Pd(PPh_3)_4$, 110 °C, N_2, 5 hrs, 72%; (ii) KOH, EtOH, H_2O, reflux, 10 hrs, 83%; (iii) TFAA-TFA, 0 °C, overnight, 75%; (iv) Fremy's salt, MeOH, 1/6 M aq. Na_2HPO_4, r. t., overnight, 86%.

Table 1
IC_{50} values of tanshinone derivatives against breast cancer lines.[#]

Compounds	IUPAC name	IC_{50} (μM) (MCF7)	IC_{50} (μM) (MDA-MB231)
1	1,6-dimethylnaphtho[1,2-*g*][1]benzofuran-10,11-dione	7.927 ± 0.37	7.962 ± 1.28
2	1,6,6-trimethyl-8,9-dihydro-7H-naphtho[1,2-*g*][1]benzofuran-10,11-dione	7.7935 ± 1.27	7.695 ± 0.176
15	Phenanthro[2,1-*b*]furan-10,11-dione	14.411 ± 2.65	20.875 ± 1.68
23	Phenanthro[3,4-*b*]furan-4,5-dione	15.7625 ± 3.062	17.45 ± 3.12
25	Phenanthro[4,3-*b*]thiophene-4,5-dione	12.7865 ± 0.81	15.61 ± 3.01
27	10-methoxyphenanthro[3,4-*b*]thiophene-4,5-dione	8.02 ± 0.91	6.00 ± 0.28
36	9-methylnaphtho[1,2-*b*:7,8-*b*']bisthiophene-4,5-dione	17.5225 ± 0.53	23.4285 ± 7.84
43	9-methylnaphtho[2,1-*b*:7,8-*b*']bisthiophene-4,5-dione	14.566 ± 2.85	20.565 ± 2.59
48	naphtho[1,2-*b*]thiophene-4,5-dione	1.945 ± 0.06	2.595 ± 1.03
52	naphtho[2,1-*b*]thiophene-4,5-dione	1.8565 ± 0.10	2.955 ± 1.18

[#] Cells were treated with indicated compounds for 24 h and the cell viability was determined by MTT assay. Each experiment was independently repeated three times.

chemotherapeutic agents.[39–41] Accordingly, in many human cancers including breast cancer autophagy induction potentially contributes to attain drug resistance through counteracting apoptosis triggered during chemotherapy.[41–43] Research suggests that autophagy induction appears to play a dual role in both luminal and triple negative breast cancers.[44] For example, tetrandrine, a bis-benzylisoquinoline alkaloid, promotes autophagy mediated cell death in MCF7 line.[45] Additionally, a growing body of evidence suggested that natural tanshinones and their derivatives induce cell death in multiple cancer cell lines through manipulating autophagy pathway.[46–49] Mechanistically, both apoptosis and autophagy cascades share regulatory mechanisms essentially controlled by Bcl-2 family members, where anti-apoptotic proteins Bcl-2 (*BCL2*) or Bcl-xL (*BCL2L1*) block apoptosis and autophagy by sequestering primarily two other family members BH3-only proteins - pro-apoptotic Bim (*BCL2L11*) and pro-autophagic Beclin 1 (*BECN1*).[50–53] Collectively, Bim and Beclin 1 appear to play central roles in regulating the balance between autophagy and apoptosis, which in turn decides cancer cell death or cell survival in response to chemotherapeutic agents.[50]

The previous results indicated that compounds **48** and **52** caused cell death partly by apoptotic induction. We next wondered that whether compounds **48** and **52** induced cell apoptosis through mitochondrial regulation of Bcl-2 family member proteins (Fig. 6**A**). While there was no change of pro-apoptotic Bcl-2 proteins including Bax and Bak along with anti-apoptotic Bcl-2 proteins such as Bcl-2 and Bcl-xL, the relative level of pro-apoptotic Bim expression was dramatically increased in response to all three tanshinone derivatives compounds **27**, **48** and **52** in MCF7 cells (Fig. 6**A**). Furthermore, compounds **48** and **52**, but not **27** induced the pro-autophagic Bcl-2 family member protein Beclin 1 (Fig. 6**A**). Upon various cellular insults, Beclin 1 initiates autophagosme formation[54] and thus it does not indicate true completion of autophagy pathway (known as autophagy flux), where the sequestered cytoplasimic materials are degraded after fusion between autophagosomes and lysosomes.[55] When autophagy is triggered, cleavage of LC3-I to LC3-II occurs with the assistance of ATG3 and ATG7. Accumulation of lipidated LC3-II leads to formation of a complex of ubiquitin-like system consisting of ATG5, ATG12 and ATG16, which further helps in the autophagosome formation. p62 (*SQSTM1*) is an adaptor protein, which binds to the autophagosomal membrane along with LC3-II and delivers the ubiquitinated cytoplasmic cargo for degradation within the autolysosome (a fusion between autophagosome and lysosomal structure).[55,56] Moreover, p62 is itself degraded and represents a good indicator for autophagy flux.[56–58] Western blot analyses clearly demonstrated that compounds **27**, **48** and **52** treatment in MCF7 cells significantly enhanced ratio of LC3-II:LC3-I (densitometric analyses of LC3-II cleavage over LC3-I) as well as p62 degradation (Fig. 6**A**). To further substantiate this data, MCF7 cells transiently transfected with GFP-tagged-LC3 expressing plasmid were either left untreated (DMSO control) or treated with 2.5 μM tanshinones and their three analogues. 24 h post-treatment the cells were stained with lyso-tracker and hoechest and viewed under confocal microscope (Fig. 6**B**). Live cell confocal microscopy revealed drastic amplification of LC3 puncta formation (lipidated LC3-II attached with the autophagosmal membrane) coincided with lysosomes in response to all three tanshinone derivatives compounds **27**, **48** and **52** treatment as compared to DMSO control and two parent natural tanshinones, compounds **1** and **2** (Fig. 6**B**), indicating that tanshinone analogues might deregulate autophagy pathway.

In response to various stresses autophagy is activated independent or dependent of transcriptional regulation.[57,59,60] In order to determine the underlying mechanisms of compounds **48** and **52** induced autophagy pathway, real time PCR analyses were carried out using total RNA extracted from MCF7 cells either left untreated (DMSO control) or treated with 2.5 μM tanshinones and three derivatives for 24 h (Fig. 6**C**). The real time PCR profiled a total of thirty four key regulatory genes that are critically involved in regulating the autophagy pathway as described in **Table S1**. The primer sequences for this study are listed in **Table S2**. The relative expression (ΔCt value) of each transcript from average value of three housekeeping genes including *ACTB, B2M* and *GAPDH* was represented as heatmap (log2) using $2^{-\Delta\Delta Ct}$ method after normalization of the raw data in respect to DMSO treated MCF7 cells (Fig. 6**C**). The results demonstrated that as similar to western blot analyses, treatment of all three tanshinone derivatives compounds **27**, **48** and **52** along with Tan-IIA (**2**) transcriptionally activated pro-apoptotic Bcl-2 family member *BCL2L11* gene expression (Fig. 6**C**). Among other pro-apoptotic Bcl-2 family members, although to a lesser extent, treatments of compounds **48** and **52** led to a specific transcriptional activation of *BAD* gene (Fig. 7**C**). In general, compound **48** as compared compound **52** appeared to be more potent transcriptional activator. A number of autophagy related genes including *ATG16L1*, *ATG16L2*, *GABARAP*, *GABARAPL1*, *GABARAPL2*, *PIK3CG*, *UVRAG* involved in autophagosome biogenesis were significantly up-regulated in compounds **48** and **52** treated cells (Fig. 6**C**). In addition, compound **48** and **52** treatment transcriptionally activated two unfolded protein response (UPR) genes *DDIT3* (CHOP) and *PPP1R15A* (GADD34) (Fig. 6**C**). Taken together, the above results suggested that compounds **48** and **52** might induce cell death by promoting autophagy flux through transcriptional activation of genes involved in autophagosome formation under stress conditions.

Compounds 48 and 52 transcriptionally activate UPR regulators in MCF7 cells: Owing to aberrant cell proliferation as well as in response to various cell stresses such as growth factor deprivation and chemotherapy, cancer cells often encounter endoplasmic reticulum stress as a consequence of accumulation of mis-folded and un-folded proteins.[61,62] This initiates an Unfolded Protein Response (UPR) triggered by three tarnsmembrane receptors - PERK (*EIF2AK3*), ATF6 and IRE1 (*ERN1*) signaling cascades.[61,63] In order to alleviate the UPR response, autophagy is subsequently activated in which the mis-/un-folded protein aggregates are degraded and allows cancer cells to grow in such a hostile conditions by providing free amino acids as energy resource.[61,64] However, in case of prolonged stress conditions, UPR

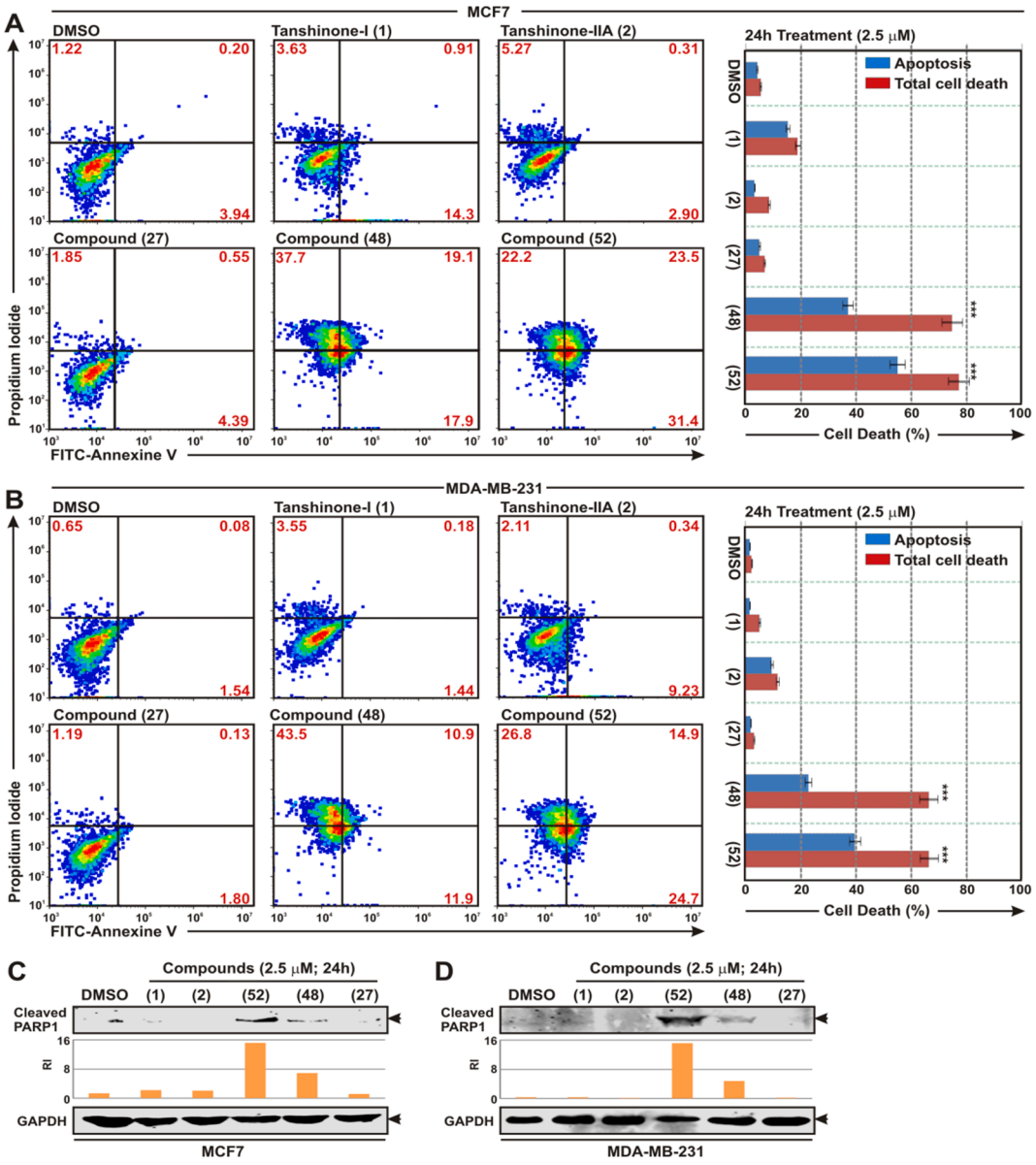

Fig. 5. Cell death induced by tanshinones (**1** and **2**) and their derivatives - compounds **27**, **48** and **52**: ~0.5 × 10^5 (A) MCF7 and (B) MDA-MB-231 cells plated into each well of six-well plates were either left untreated (DMSO control) or treated with 2.5 μM natural tanshinones (compounds **1** and **2**) and their three derivatives (compounds **27**, **48** and **52**) for 24 h were subjected to apoptosis assay using annexin V/propidium iodide (PI) staining. FITC labeled annexin V binding (Ex = 488 nm; Em = 350 nm) and PI staining were detected using BD Accuri C6 Flow Cytometry Analyzer. Error bars represent standard deviations of duplicate assays of two independent experiments. *, **, *** = p-value < 0.01, 0.005 and 0.001 respectively. ~5 × 10^6 (C)**** MCF7 and (D) MDA-MB-231 cells treated with drugs using a similar experimental set up, were subjected to western blot analyses with the indicated antibodies. GAPDH blot was used as loading control and protein bands were quantified by Odyssey imager software and indicated as bar diagrams at the bottom of corresponding lanes.

triggers apoptotic cell death by activating a number of death regulators.[63,65] PERK-mediated eIF2α phosphorylation leads stabilization of the transcription factor ATF4, which in turn triggers transcriptional activation of several genes involved in both autophagy and apoptosis.[66,67] Among these, CHOP (CEBP (CCAAT/enhancer-binding protein) homologous protein/growth arrest and DNA-damaged-inducible protein 153 or GADD153) transcription factor plays a dual role in both inducing apoptosis and limiting autophagy through the transcriptional control of specific downstream target genes in response to cellular stress signals.[68,69] In contrast, PPP1R15A (Growth arrest and DNA damage-inducible protein 34 or GADD34), which is also activated by PERK-eIF2α-ATF4 pathway, negatively regulates this cascade via a feedback mechanism by inducing eIF2α dephosphorylation.[70] Moreover, GADD34 plays an essential role in autophagy during stress conditions and initiates translation of several genes required for lysosomal biogenesis and to maintain autophagy flux.[71] As described in Fig. 6**C**, compounds **48** and **52** mediated specific transcriptional activation of CHOP (*DDIT3*) and GADD34 (*PPP1R15A*) as well as to comprehend possible mechanism of dual apoptosis and autophagy induction, led us to further explore the overall transcriptional changes in UPR and related pathway in response to these compounds. To this end, total RNA was isolated from MCF7 cells with or without the treatment with compounds **48** and **52** for 24, cDNA was prepared and subjected to PCR microarray analyses (Fig. 7**A**), which profiles a total of 84 key regulatory genes that are critically involved in regulating the UPR signalling cascade as described in **Table S3**. As described in the **Experimental Section**, in response to compounds **48** and **52** treatment, the relative expression (ΔCt) of each transcript from average value of five housekeeping genes (*ACTB, B2M, GAPDH, HPRT1 and RPLP0)* in the array platform was represented as heatmap (log2) using $2^{-\Delta\Delta Ct}$ method after normalization

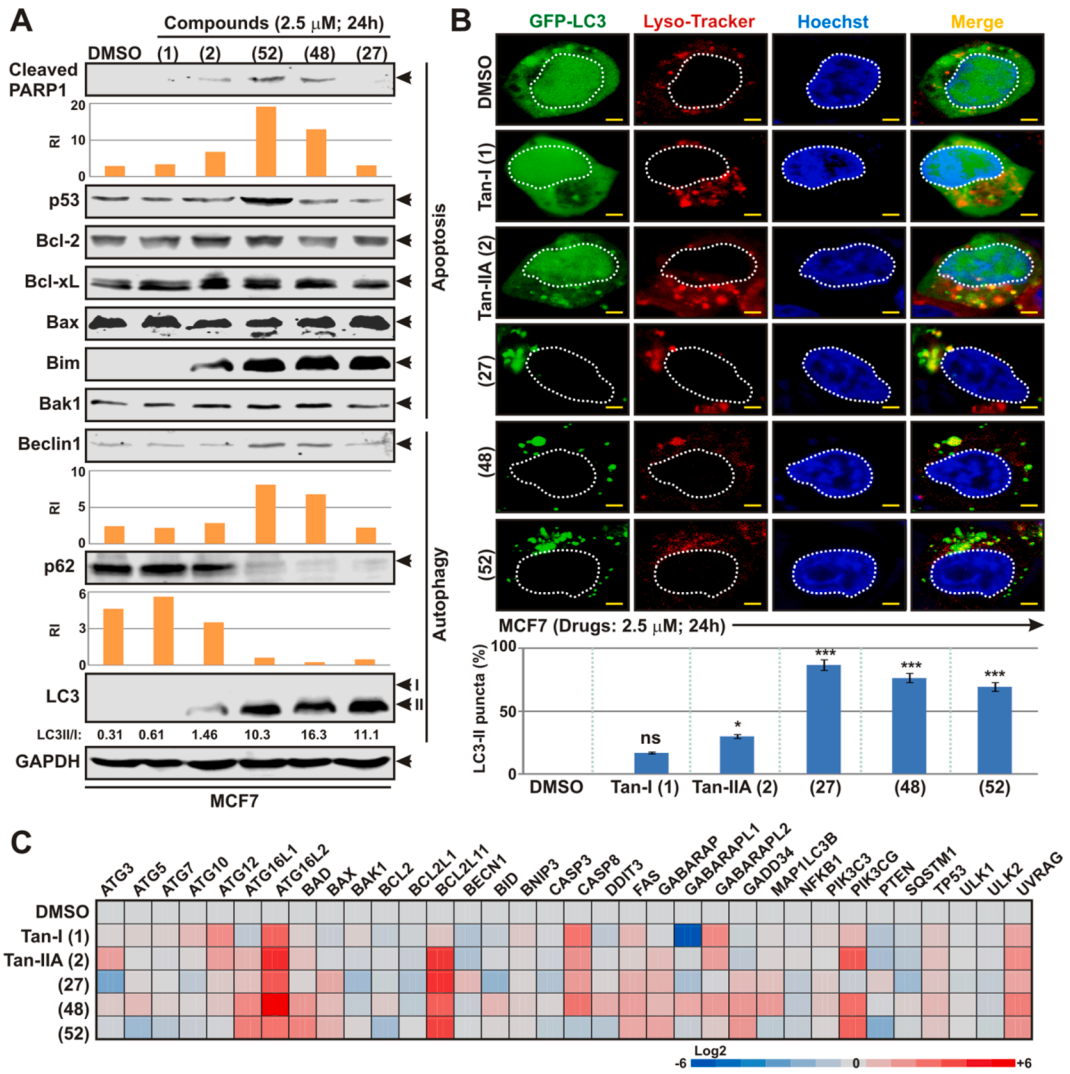

Fig. 6. Compounds **48** and **52** induce both apoptosis and autophagy: (A) ~5 × 10^6 MCF7 cells either left untreated (DMSO control) or treated with 2.5 μM natural tanshinones (compounds **1** and **2**) and their three derivatives (compounds **27**, **48** and **52**) for 24 h were subjected to western blot analyses with the indicated antibodies. Protein band intensities in were quantified by Odyssey imager software and indicated either as bar diagrams or LC3-II/I ratio at the bottom of each corresponding lane. Representative gel pictures are shown of two independent experiments. GAPDH blot was performed as loading control. (B) ~1 × 10^6 MCF7 cells grown at 70% confluency on 35 mm dish embedded with 12 mm glass viewing areatransiently transfected with GFP-LC3 expressing construct were either left untreated (DMSO control) or treated with 2.5 μM drugs for 24 h as stated above and subjected for live cell confocal microscopy. Nuclei and lysosomes were counterstained with Hoechst 33,342 and LysoTracker Red DND-99, respectively. Each panel of confocal images is representative pictures of two independent experiments. Scale bars, 5 μm. The bar diagrams below represent the mean value of LC3 puncta counting from at least 10 cells of 3 different fields. Error bars represent standard deviations of duplicate assays of two independent experiments. *, **, *** = p-value < 0.01, 0.005 and 0.001, respectively. ns = non significant. (C) Using the similar experimental set up as described in (A), total RNA was isolated and subjected to cDNA preparation followed by quantitative real-time PCR (qPCR) analyses for the selected cell genes. The relative changes in transcripts (log2) using the $2^{-\Delta\Delta Ct}$ method are represented as heatmap in comparison to DMSO control using GAPDH, B2M and RPLPO as housekeeping genes. Two independent experiments were carried out in similar settings and results represent as an average value for each transcript.

of the raw data in respect to DMSO treated cells (Fig. 7**A**). The results demonstrated that along with *DDIT3* and *PPP1R15A*, several UPR regulators particularly the IRE1 signalling cascade were transcriptionally activated in response to the drug treatment (Fig. 7**A**). Western blot analyses further validated the expressions of ATF4, CHOP and GADD34 in drug treated cells as compared to the DMSO control (Fig. 7**B**). Overall, the results revealed that compounds **48** and **52** stimulate cell death by manipulating autophagy-UPR network particularly inducing expression of several death regulators – GADD34 and CHOP.

Compounds 48 and 52 promote autophagy mediated cell death: Hitherto, the results pointed towards a model that compounds **48** and **52** might regulate cell death through enhancing autophagy flux. Indeed, both compounds **48** and **52** induced apoptosis (PARP cleavage) and autophagy flux (LC3-II conversion and p62 degradation) simultaneously in a dose dependent fashion (Fig. 8**A and 8C**). In order to establish the notion of autophagy mediated cell death, MCF7 cells treated with 2.5 μM either compound **48** or **52** were further treated with an autophagy inhibitor, chloroquine (CQ) (Fig. 8**B and 8D**). The anti-malarial drug CQ blocks autophagy flux by escalating the lysosomal acidic pH and blocks the fusion between autophagosome and lysosome, which in turn leads to inhibition of p62 degradation and accumulation of lipidated LC3-II forms.[58,72] In fact, the results demonstrated that CQ co-administration resulted in significant reduction (~2-fold) of cell apoptosis (decreased cleaved PARP1 expression) induced by either compounds **48** or **52** alone (Fig. 8**B and 8D**). Effect of CQ, was further demonstrated by accumulation of autophagy markers both p62 and LC3 cleavage in western blot analyses (Fig. 8**B and 8D**). Additionally, live cell confocal microscopy analyses of MCF7 cells transiently co-transfected with plasmids

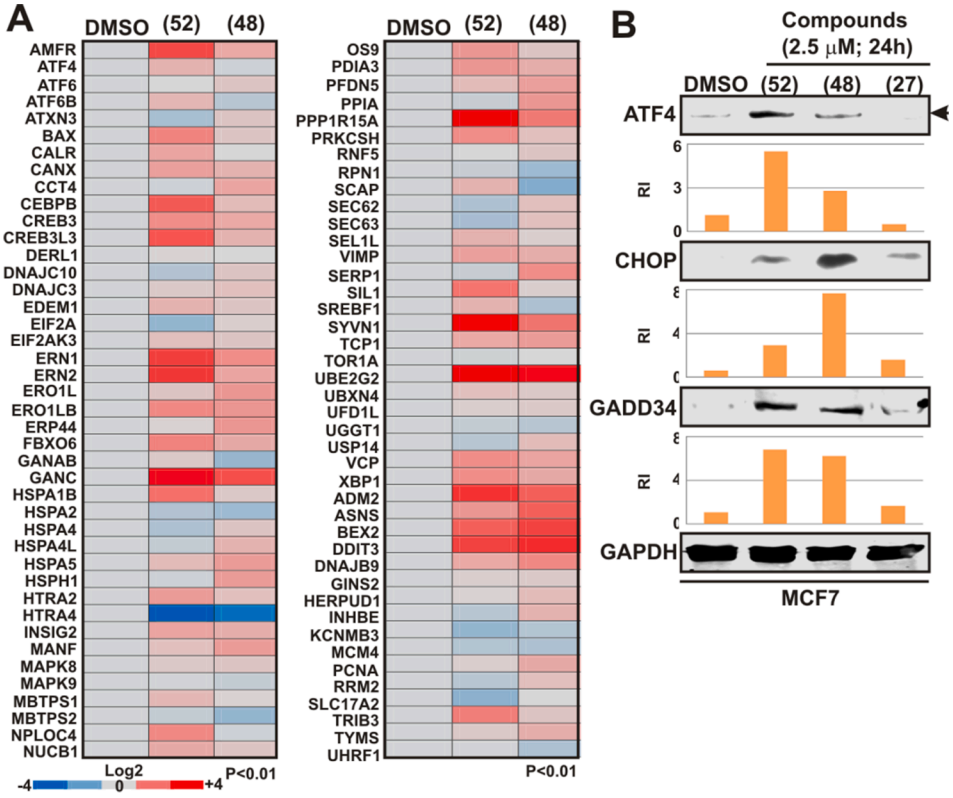

Fig. 7. Compounds **48** and **52** transcriptionally activate UPR regulators: ~10 × 10^6 MCF7 cells either left untreated (DMSO control) or treated with 2.5 μM compounds **48** or **52** for 24 h, were harvested for either total RNA extraction followed by cDNA generation according to manufacturer's protocol or protein extraction for western blot analyses. (A) Amplified cDNAs were then subjected to PCR-microarray analyses for "Unfolded Protein Response (UPR)" pathway from SABiosciences in accordance with manufacturer's instructions. The relative changes in transcripts (log2) using the $2^{-\Delta\Delta Ct}$ method were represented as a heat map in comparison to control cells taking average of five housekeeping genes *ACTB*, *B2M*, GAPDH, HPRT1 and *RPLP0*. Data analysis (algorithm provided by the manufacturer) also incorporated the quality check to include or exclude the real-time PCR data points for individual genes. Two independent experiments were carried out in similar settings and results represent as an average value for each transcript. (B) Western blot analyses were carried out using the indicated antibodies. Protein band intensities (pixels) in each lane were quantified by Odyssey imager software and presented as either by bar diagrams at the bottom of each picture.

expressing GFP-tagged LC3 and mCherry-tagged p62 in response to individual treatment of tanshinone analogues and CQ clearly revealed that both compounds **48** and **52** significantly induced distinct puncta pattern of GFP-LC3 molecule co-localized with reduced mCherry-p62 expression as compared CQ treatment alone (Fig. 8**E**).

In order to further establish whether these thiophene analogues of natural tanshinones could induce autophagy mediated cell death, we performed cell viability assays in both MCF7 and MDA-MB-231 cells individually treated with 2.5 μM compounds **48** and **52** with increasing doses (25, 50 and 100 μM) of CQ for 24 h (Fig. 8**F and 8G**). Although CQ treatment alone caused cell death due to its well-known cytotoxity at higher doses (100 μM), it significantly inhibited cell-killing activities exerted by compounds **48** and **52** in a dose dependent fashion (Fig. 8**F and 8G**). In agreement to this, previously Tan-IIA demonstrated autophagy mediated cell death in human osteosarcoma MG-63 cells at higher doses and the effect could be somewhat alleviated in the presence of CQ.[7] Taken together, the results above evidently demonstrated that the two novel thiophene analogues - compounds **48** and **52** are potent autophagy inducers and thereby promoting cell death.

3. Conclusions

In sum, we successfully synthesized a total of eight novel phenanthraquinones derivatives with thiophene and furan moieties as tanshinone analogues through utilizing diversity-oriented synthesis[73], a synthetic approach that engages efficient incorporation of multiple molecular scaffolds in the library for the discovery of novel biologically active small molecules. Some modifications were made in the ring A or both ring A and D of the core nucleus present in natural occurring furophenanthraquinone: Isotanshinone-II. In addition, we also prepared two novel thienonaphthoquinone derivatives **48** and **52** by simulating BCD ring of Isotanshinone-II core nucleus *via* a novel synthetic route. Overall, our study supports the notion of development of two thiphene analogues - compounds **48** and **52** towards the treatment of breast cancer through modulating autophagy pathway. Given the growing appreciation of natural products in drug discovery together with potential anticancer properties of natural tanshinones, the markedly improved anti-proliferative activities of tanshinone analogues - compounds **48** and **52** merit further meticulous investigations for successful development as anticancer agents. In addition to elucidating the underlying molecular mechanism of autophagy mediated cell death, thorough *in vivo* studies need to be conducted for further validation as well as to establish the optimal dose for potential therapeutic application. Moreover, toxicological studies should be performed to envisage both short-term and long-term possible side effects. Furthermore, studies to assess bioavailability, pharmacokinetics, and pharmacodynamics need be carried out in order to ultimately develop the two thiophene analogues as anticancer drugs against various subtypes of breast cancers.

4. Experimental section

General Procedures: All reactions were carried out using oven-dried or flame dried clean glass wares. All reagents were purchased from commercial suppliers in the highest purity grade available and used without further purification. The solvents, chloroform (CHCl3), dichloromethane (DCM), diethyl ether (Et2O), ethanol (EtOH), dimethylformamide (DMF), Benzene, ethanol (EtOH), methanol (MeOH), Petroleum ether (P.E) and ethyl acetate (EtOAc) were purchased from E. Merck (India) Ltd. or SRL (India) Ltd. and distilled prior to use. P.E refers to the fraction boiling in the range 60–80 °C. All common solvents and reagents (CHCl3, DMF, Et3N, benzene, *s*-collidine, etc.) were dried as per literature procedure. Furanboronic acids, thiophene boronic acids, 1-tetralone, 4-methyl-1-tetralone, 6-methoxy-1-tetralone, cyclohexanone, cyclopentanone, cyclooctanone, 4-*tert*-butylcyclohexanone, tetrakis(triphenylphosphine)palladium(0), 2,3-dichloro-5,6-dicyanobenzoquinone (DDQ), $CDCl_3$ and DMSO-d_6 were purchased from Sigma Aldrich (now Merck). Trifluoroacetic anhydride (TFAA), trifluoroacetic acid (TFA), phosphorous tribromide, Pd/C, sodium borohydride ($NaBH_4$), Mesyl chloride and *s*-collidine were purchased from

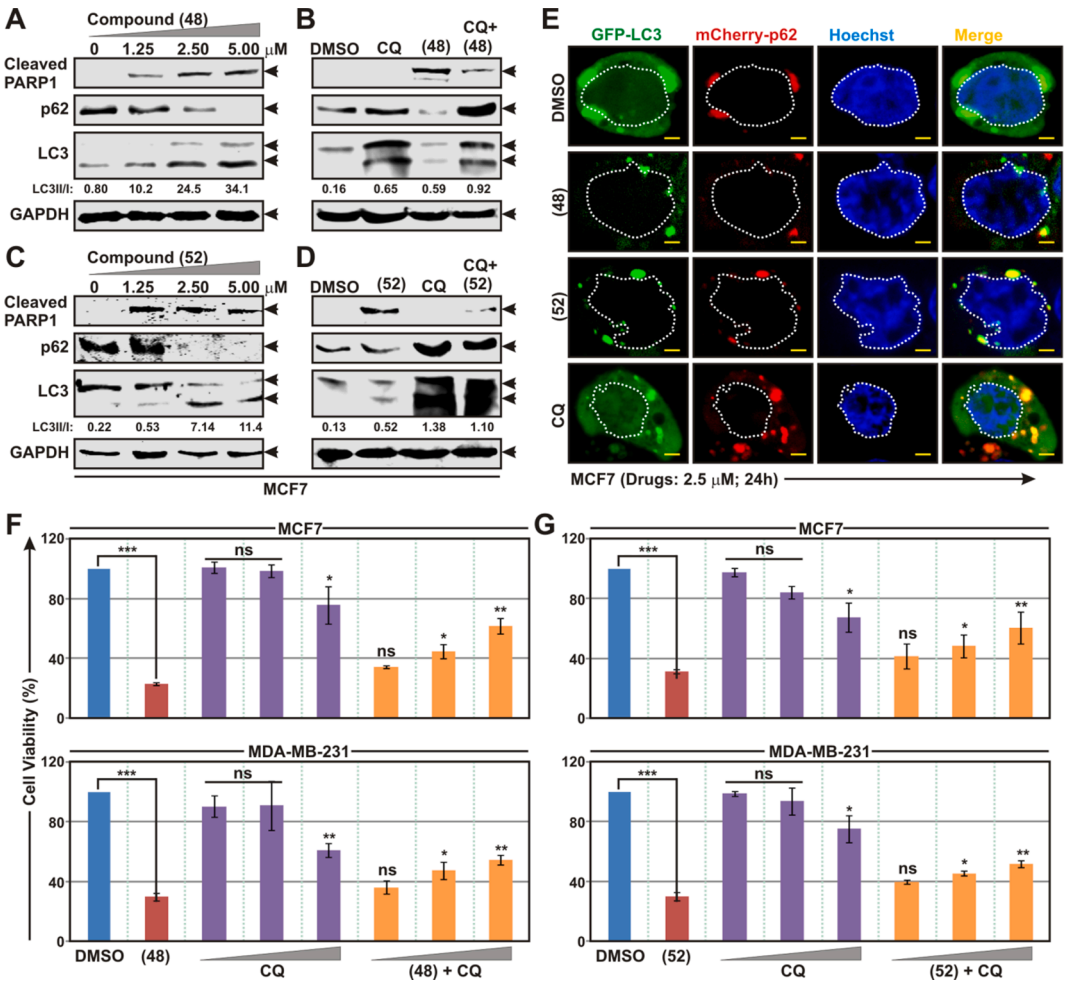

Fig. 8. Compounds **48** and **52** promote autophagy mediated cell death: ~5 × 10^6 MCF7 cells were either left untreated (DMSO control) or treated with increasing doses (0, 1.25, 2.5 and 5 μM) of compounds (A) **48** or (C) **52**. Using a similar experimental setting, MCF7 cells were either individually treated with 2.5 μM compounds (B) **48** or (D) **52** or in combination with 50 μM Chloroquine (CQ). (A-D) 24 h post-treatment cells were harvested and subjected to western blots were performed with the indicated antibodies. GAPDH blot was performed as loading control. The relative intensities of LC3 protein bands were quantified using the software provided by Odyssey CLx Imaging System and shown as LC3-II/I ratio at the bottom of LC3 blot Representative gel pictures are shown of at least two independent experiments. (E) ~1 × 10^6 MCF7 cells transiently transfected with constructs expressing GFP-LC3 and mCherry-p62 for 24 h were left untreated (DMSO control) or treated with 2.5 μM compounds **48** or **52** or 50 μM CQ for another 24 h and subjected to live cell confocal microscopy after staining the nucleus with Hochest 33342. Each panel in (E) corresponds to single experiment of two independent experiments. Scale bars, 5 μm. (F-G) ~0.5 × 10^5 MCF7 and MDA-MB-231 cells plated into each well of six-well plates were either left untreated (DMSO control) or treated with 2.5 μM compounds (F) **48** or (G) **52** in the presence and absence of increasing concentrations (25, 50 and 100 μM) of CQ for 24 h at 37 °C in a humidified CO_2 chamber and subjected cell viability assays using MTT as described in the Experimental Section. Error bars represent standard deviations of duplicate assays of two independent experiments. *, **, *** = p-value < 0.01, 0.005 and 0.001, respectively. ns = non significant.

Spectrochem, India. Fremy's salt (potassium nitrosodisulfonate) was prepared in the laboratory as per literature procedure. Anhydrous sodium sulfate (Na_2SO_4) was used for drying solutions.

Purification by column chromatography was done using silica gel (100–200 mesh, 230–400 mesh) (E. Merck, India or SRL) using P.E 60–80 °C and EtOAc as eluents, unless otherwise mentioned. Pre-coated silica gel 60 GF254 TLC sheets on aluminium plate (E. Merck, Germany) were used for thin-layer chromatography (TLC). Melting points were recorded in open capillaries using conc. H_2SO_4 bath or electrical melting apparatus and are uncorrected.

Infrared spectra were recorded on KBr pellets using a Shimadzu Fourier Transform

(FT-IR) 8300 spectrophotometer to confirm the presence of the main functional groups present in each of the synthesized tanshinone analogs. ^{1}H NMR (500 MHz or 400 MHz or 300 MHz) and ^{13}C NMR (125 MHz or 100 MHz or 75 MHz) spectra were recorded on a Bruker AVANCE III 500 MHz or 400 MHz or 300 MHz NMR spectrometer using tetramethylsilane as the internal standard. The ESIMS was recorded on a JEOL JMSAX505HA. High-resolution-mass spectra (HRMS) were recorded on either a TRACE GC ULTRA POLARIS Q or a Waters Qtof Micro YA263 mass spectrometer. All compounds tested in biological assays are >95% pure.

(2-Furan-3-yl-naphthalen-1-yl)-acetic acid methyl ester (12): 0.16 g (1.42 mmol) 3-furanboronic acid, 1 ml (7.2 mmol) triethylamine and 0.016 g (1–2 mol%) $Pd(PPh_3)_4$ were added to a solution of 0.300 g (1.08 mmol) compound **11** in 3 ml DMF. Now, the reaction mixture was allowed to heat at 110 °C with constant stirring under argon atmosphere for about 7 hr. After cooling to room temperature, it was poured into ice cold water and extracted with ether. The ether layer was washed with 10 ml ice cold 5% $NaHCO_3$ solution followed by 10 ml ice cold 5% brine solution. It was collected and dried over anhydrous Na_2SO_4 and solvent was removed. The collected compound was purified by column chromatography over silica gel (230–400 mesh) (EtOAc: P.E = 10:90). The compound solidified in presence of ethanol (yield 0.200 g, 70%). M.p: 75–77 °C. IR: 1750 cm^{-1}. ^{1}H NMR (400 MHz, $CDCl_3$): δ 7.90–7.92 (m, 1H), 7.72–7.80 (m, 2H), 7.56–7.57 (m, 1H), 7.37–7.50 (m, 4H), 6.54 (d,

1H, J = 2.4 Hz), 4.11 (s, 2H), 3.64 (s, 3H). MS (QTOF ES+): found, 267.0729 $[M+H]^+$; calcd for $C_{17}H_{15}O_3$, 267.1021.

3-(2-Furan-3-yl-naphthalen-1-yl)-acetic acid (13): 1 ml of 20% aqueous KOH solution was added to a solution of 0.20 g (0.75 mmol) of the compound **12** in 3 ml ethanol and was allowed to reflux for 9 hr. The reaction mixture was quenched with some crushed ice water, acidified with cold concentrated HCl and filtered. The collected residue was dissolved in 5–10 ml saturated solution of $NaHCO_3$ and further acidified with cold conc. HCl. The white solid appeared was filtered, the residue was washed with ice cold water and collected (0.14 g, 74%) M.P: 160 °C. IR: 1690 cm^{-1}. MS (QTOF ES+): found, 253.0873 $[M+H]^+$; calcd for $C_{16}H_{13}O_3$, 253.0865.

Phenanthro [2,1-*b*] furan-11-ol (14): 0.07 g (0.28 mmol) of compound **13**, 0.89 ml trifluoroacetic anhydride and 0.18 ml trifluoroacetic acid was allowed to react at room temperature for overnight. It was then poured into ice cold saturated solution of $NaHCO_3$, stirred well, extracted with DCM. The organic layer was collected, washed with cold $NaHCO_3$ solution, finally dried over anhydrous Na_2SO_4 and solvent removed. The compound (a faint brown solid) was purified by column chromatography (silica gel/230–400 mesh and benzene as elluent) (yield 0.05 g, 75%), m.p: 98 °C. IR: 1240, 1590, 3430 cm^{-1}. ^1H NMR (400 MHz, $CDCl_3$): δ 8.57 (d, 1H, J = 8.4 Hz), 8.09 (s, 1H), 7.61 (ddd, 1H, J = 6.8 Hz), 8.0 (d, 1H, J = 8.8 Hz), 7.92 (d, 1H, J = 8 Hz), 7.75–7.80 (m, 2H), 7.55–7.62 (m, 2H), 7.32 (d, 1H, J = 2 Hz). MS (QTOF ES+): found, 235.0864 $[M+H]^+$; calcd for $C_{16}H_{11}O_2$, 235.0759.

Phenanthro [2,1-*b*] furan-10,11-dione (15): To an aqueous solution of 14 ml 1/6 M of Na_2HPO_4, 0.170 g (0.63 mmol) of Fremy's salt was added and stirred at 0 °C. Now, to this stirred solution, a solution of the compound **14** (0.05 g, 0.21 mmol) in MeOH (7 ml) was added drop wise. The reaction mixture was allowed to stir at 0–5 °C for 4 hr and then left in the freeze for overnight. The dark red solid was filtered, washed with 5 ml ice cold water and collected. The fluorescent orange compound was crystallized with benzene (yield 0.03 g, 57%), m.p greater than 200 °C. IR: 770, 1050, 1430, 1600, 1650 cm^{-1}. ^1H NMR (400 MHz, DMSO-d_6): δ 9.43 (d, 1H, J = 8.8 Hz), 8.12 (d, 1H, J = 8 Hz), 7.80–7.84 (m, 2H), 7.63–7.73 (m, 2H), 7.52–7.56 (m, 1H), 6.98 (s, 1H). ^{13}C NMR (100 MHz, $CDCl_3$): δ = 170.9, 167.1, 152.6, 137.2, 136.9, 134.3, 132.4, 132.2, 130.9, 129.8, 128.8, 127.4, 126.0, 124.4, 123.5, 110.2 ppm. MS (QTOF ES+): found, 249.0634 $[M+H]^+$; calcd for $C_{16}H_9O_3$, 249.0552.

1-(3-furyl)-2-naphthaldehyde (18): A mixture of the bromoaldehyde **17** (0.235 g, 1.0 mmol), 3-furanboronic acid (0.155 g, 1.2 mmol.), Et_3N (0.5 ml, 3.5 mmol) and DMF (2 ml) was stirred under argon for 30 min. $Pd(PPh_3)_4$ (2 mol%) was added to it. The mixture was then heated with stirring under argon at 100 °C until (10 hr) the reaction was completed. The reaction mixture was then cooled to r.t, poured into ice-cold water and extracted with ether (3 × 20 ml). The organic layer was washed successively with aq. $NaHCO_3$, brine and dried. Removal of the solvent afforded the crude product which was purified by column chromatography, followed by recrystalisation from Pet Ether to furnish an orange solid. Yield 0.135 g, 61%. M.p 86–88 °C. IR (νmax, cm^{-1}): 1671; ^1H NMR (400 MHz, $CDCl_3$): δ 6.649 (s, 1H), 7.519 (t, 1H, J = 8.0 Hz), 7.59 (s, 1H), 7.627 (t, 1H, J = 8.0 Hz), 7.686 (d, 1H, J = 1.6 Hz), 7.904 (d, 2H, J = 8.8 Hz), 7.97 (d, 1H, J = 8.4 Hz), 8.032 (d, 1H, J = 8.8 Hz), 10.148 (s, 1H) ppm; ^{13}C NMR (100 MHz, $CDCl_3$): δ = 113.9, 122.2, 127.0, 127.2, 128.3, 128.6, 128.9, 142.7, 143.5, 192.6, 118.6, 132.2, 132.8, 136.0, 137.2 ppm. HR-MS (ESI): calcd for $C_{15}H_{10}O_2$: 222.0681 $[M^+]$, found 222.0688.

1-(3-Furyl)-2-hydroxymethylnaphthalene (19): To the stirred solution of the aldehyde **18** (0.222 g, 1 mmol) in EtOH (10 ml), taken in a 50 ml r.b flask, $NaBH_4$ 0.04 g (1.0 mmol) was added pinch by pinch. The stirring was continued at r.t. for further 2 hrs. Excess EtOH was removed by distillation and the reaction mixture was diluted with 5 ml ice water and extracted with DCM (3 × 15 ml). The organic layer was washed thoroughly with water and dried. Removal of the solvent afforded the crude product which purified by column chromatography to furnish **19** as a colourless oil. Yield 0.217 g, 97%. IR (ν_{max}, cm^{-1}): 755, 3428. ^1H NMR (400 MHz, $CDCl_3$): δ 4.663 (s, 2H), 6.371 (d, 1H, J = 1.6 Hz), 7.24–7.44 (m, 4H), 7.436 (d, 1H, J = 1.8 Hz), 7.55–7.65 (m, 2H), 7.713 (d, 1H, J = 8.0 Hz) ppm. ^{13}C NMR (100 MHz, $CDCl_3$): δ = 62.3, 108.8, 124.8, 125.7, 127.2, 127.4, 127.5, 128.4, 138.5, 142.9, 129.3, 132.0, 132.1, 133.7, 134.7 ppm.

2-Cyanomethyl-1-(3-furyl)naphthalene (20): A mixture of **19** (0.224 g, 1.0 mmol), *s*-collidine (0.2 ml, 1.3 mmol), mesyl chloride (0.1 ml, 1.3 mmol) and lithium chloride (0.07 mg, 1.5 mmol) in DMF (8 ml) were stirred overnight at 0–5 °C under anhydrous condition. The reaction mixture was then poured into crushed ice and extracted with ether (3 × 20 ml). The organic layer was washed with ice-cold aq. 5% HCl, thoroughly with cold water and dried (anhyd. Na_2SO_4). The solvent was removed to furnish brown oil (0.174 g, 72%). This crude product (0.243 g, 1.0 mmol) was dissolved in dry DMF (2 ml), and KCN (0.1 g, 1.5 mmol) was added to it and stirred for 6 hrs at rt and then for 1 h at 50 °C. The reaction mixture was poured into ice water (5 ml) and extracted with ether (3 × 20 ml). The organic layer was washed thoroughly with ice-cold water, dried and the solvent removed. The crude product was purified by column chromatography to furnished **20** as a light yellow solid. Yield 0.177 g, 76%. M.p 116–118 °C; IR (ν_{max}): 758, 2240 cm^{-1}; ^1H NMR (400 MHz, $CDCl_3$): δ 3.747 (s, 2H), 6.494 (s, 1H), 7.453 (dt, 1H, J = 17.6 Hz & 20.8 Hz), 7.50 (d, 1H, J = 8.0 Hz), 7.51 (s, 1H), 7.59 (d, 1H, J = 8.8 Hz), 7.675 (s, 1H), 7.725 (d, 1H, J = 8.4 Hz), 7.868 (d, 1H, J = 8.0 Hz), 7.898 (d, 1H, J = 8.8 Hz) ppm. ^{13}C NMR (100 MHz, $CDCl_3$): δ = 22.7, 112.6, 125.8, 126.3, 126.4, 126.8, 128.0, 129.0, 141.2, 143.8, 118.4, 120.7, 130.0, 132.9, 133.3 ppm.

2-Carboxymethyl-1-(3-furyl)naphthalene (21): A solution of **20** (0.23 g, 1 mmol) in 30% KOH (4 ml in 10 ml EtOH) was refluxed for 18 hrs. Excess EtOH was distilled off, the residual solution was diluted with ice-cold water (5 ml) and extracted with ether (2 × 15 ml). The aq. part was acidified with aq. 5% HCl under ice cold condition, and the oil that separated was extracted with DCM (3 × 20 ml). The combined organic extract washed with cold water, dried and the solvent removed. The residue was dissolved in aq. $NaHCO_3$, acidified with aq. 5% HCl in ice-cold condition, and the separated solid was filtered. It was crystallised from PE-EtOAc to furnish **21** as a light brown solid. Yield 0.206 g, 82%. Mp: 154–156 °C. IR (ν_{max}): 1707, 3105 cm^{-1}; ^1H NMR (400 MHz, $CDCl_3$): δ 3.679 (s, 2H), 6.408 (s, 1H), 7.30–7.46 (m, 4H), 7.545 (d, 1H, J = 1.2 Hz), 7.759 (d, 1H, J = 8.0 Hz), 7.767 (d, 2H, J = 8.4 Hz) ppm; ^{13}C NMR (100 MHz, $CDCl_3$): δ = 39.3, 113.1, 125.8, 126.3, 126.4, 127.5, 127.9, 128.2, 141.4, 143.1, 121.4, 129.2, 130.1, 132.8, 177.3 ppm. HR-MS: calcd for $C_{16}H_{12}O_3$ 252.0786 $[M^+]$, found 252.0791.

Phenanthro [3,4-*b*] furan-4-ol (22): TFA (1 ml) was added slowly to a mixture of 0.075 g 58 (0.075 g, 0.30 mmol) and TFAA (3 ml) at 0 °C and the solution stirred overnight under anhydrous condition. The mixture was poured into ice-cold saturated aq. $NaHCO_3$ and extracted thoroughly with DCM (3 × 20 ml). The organic layer was washed successively with aq. $NaHCO_3$ and H_2O and dried. Removal of solvent afforded the crude product which was purified by column chromatography to furnish **22** as a yellow solid. Yield 58 mg, 83%; M.p 150–152 °C; IR (ν_{max}): 3439 cm^{-1}; ^1H NMR (400 MHz, $CDCl_3$): δ 7.315 (s, 1H), 7.58 (dt, 1H, J = 1 7.6 Hz & 2 0.8 Hz), 7.698 (dt, 1H, J = 1 8.0 Hz and 2 1.6 Hz), 7.758 (s, 2H), 7.841 (d, 1H, J = 2.0 Hz), 7.909 (d, 1H, J = 2.0 Hz), 7.946 (dd, 1H, J = 1 8.0 Hz & 2 0.8 Hz), 8.891 (d, 1H, J = 8.4 Hz) ppm; ^{13}C NMR (100 MHz, $CDCl_3$): δ = 109.1, 109.4, 124.4, 125.2, 126.1, 126.4, 127.1, 128.7, 144.8, 119.4, 123.9, 130.73, 130.76, 131.7, 141.0, 144.0 ppm.

Phenanthro [3,4-*b*] furan-4,5-dione (23): A solution of 57 (0.025 g, 0.1 mmol) in MeOH (4 ml) was added drop wise. Stirring was continued overnight at rt. The reaction mixture was then extracted with DCM, dried and the solvent removed. The crude product was purified by crystallisation from MeOH. The purified product appeared as a brick red solid. Yield 19 mg, 77%. Mp: 170–172 °C. IR (ν_{max}): 1665, 1693 cm^{-1}; ^1H NMR (500 MHz, $CDCl_3$): δ 7.464 (br s,1H), 7.68 (d, 1H, J = 9.5 Hz), 7.671 (d, 1H, J = 9.5 Hz), 7.86–7.93 (m,3H), 8.184 (d, 1H, J = 8.5 Hz), 8.52–8.57 (m, 1H) ppm; ^{13}C NMR (100 MHz, $CDCl_3$): δ = 112.3, 125.2,

125.3, 128.3, 129.2, 129.5, 130.2, 150.6, 128.6, 128.8, 129.9, 135.2, 137.7, 166.9, 181.3 ppm; HRMS: calcd for $C_{16}H_8O_3$: 248.0473 [M^+], found 248.0472.

4-Bromo-6,7-dihydro-2-methylbenzo [*b*] thiophene-5-carbaldehyde (29): 2.3 ml PBr_3 (24.4 mmol) was added drop wise to an ice cold mixture of 2.5 ml DMF (27.2 mmol) in 10 ml chloroform at 0–5 °C and the stirring was continued for 30 min protecting from moisture. A solution of 2-methyl-6,7-dihydrobenzo[*b*]thiophen-4(*5H*)-one (**28**) (1.28 gm, 7.7 mmol) in 5 ml chloroform was added drop wise to it. The reaction mixture was gradually allowed to attain r.t. and stirring was continued for another 16 hrs when the reaction was found to be completed. It was poured into ice cold saturated sodium acetate solution, stirred well for about 5 min and extracted with chloroform (3 × 20 ml). Combined chloroform layer was washed successively with cold brine solution, $NaHCO_3$ solution and finally with brine solution and dried (anhyd. Na_2SO_4). After removal of the solvent, resulting crude product was purified by column chromatography [silica gel. (100–200 mesh) / P.E (60–80 °C)-EtOAC: 1:50] to obtain the title compound **29** as light yellow solid. Yield 1.45 gm (73%), mp: 70–72 °C; IR (KBr) ν_{max}: 1634 cm^{-1}; ^1H NMR (400 MHz, $CDCl_3$): $\delta = 2.38$ (s, 3H), 2.69–2.64 (m, 2H), 2.79–2.75 (m, 2H) 6.90 (s, 1H), 9.97 (s, 1H) ppm; ^{13}C NMR (100 MHz, $CDCl_3$): δ = 15.2, 22.5, 23.9, 124.7, 129.1, 135.3, 135.6, 137.1, 142.0, 192.4 ppm; HRMS (ESI+): *m/z* $[M+H]^+$ calcd. for $C_{10}H_{10}O^{81}Br$: 258.9615; found: 258.9158.

6,7-Dihydro-2-methyl-4-(2-thienyl)benzo [*b*] thiophene-5-carbaldehyde (30): 700 mg (2.69 mmol) the bromoaldehyde **29** was subjected to Suzuki coupling reaction (reaction time 10 hrs) with 2-thiopheneboronic acid (410 mg, 3.2 mmol) under the identical reaction condition, as used previously, afforded the compound **30** as orange yellow solid after usual work up and purification. Yield: 430 mg (1.65 mmol, 61%), mp: 54–56 °C; IR (KBr) ν_{max}: 1645 cm^{-1}; ^1H NMR (400 MHz), ($CDCl_3$): $\delta = 2.37$ (s, 3H), 2.78–2.83 (m, 2H), 2.83–2.91 (m, 2H), 6.52 (s, 1H), 7.0 (d, 1H, $J = 3.2$ Hz), 7.09 (d, ill split, $J \sim 5$ Hz, 1H), 7.46 (dd, $J = 4.8$ Hz & 1.6 Hz, 1H), 9.75 (s,1H) ppm; ^{13}C NMR (75 MHz, $CDCl_3$): $\delta = 15.1$, 21.8, 22.6, 124.1, 126.9, 127.5, 130.2, 131.8, 135.8, 135.9, 136.7, 141.3, 143.5, 192.2 ppm; HRMS (ESI+): *m/z* $[M+H]^+$calcd for $C_{14}H_{13}OS_2$: 261.0330; found: 261.1271 & $[M+Na]^+$ calcd for $C_{14}H_{12}NaOS_2$: 283.0227; found: 283.1413.

2-Methyl-4-(2-thienyl)benzo [*b*] thiophene-5-caraldehyde (31): 420 mg (1.61 mmol) of compound **30** and 440 mg (1.94 mmol) of DDQ in 20 ml dry benzene was refluxed (24 hrs) protecting from moisture and after usual work up,furnished the compound **31** as pale yellow solid. Yield: 360 mg (1.40 mmol, 86%), mp: 104–106 °C; IR (KBr) ν_{max}: 1676 cm^{-1}; ^1H NMR (400 MHz, $CDCl_3$): $\delta = 2.47$ & 2.50 (both s, total 3H), 6.95 (br s, 1H), 7.09 and 7.1 (both d, ill split, $J = 4.8$ Hz, total 1H), 7.13 & 7.14 (both d, $J = 3.2$ Hz, total 1H), 7.46 & 7.48 (both br s, ill split, total 1H), 7.78 (d, $J = 8.8$ Hz, 1H), 7.83 (d, $J = 8.4$ Hz, 1H), 9.97 (s, 1H) ppm; ^{13}C NMR (75 MHz, $CDCl_3$): $\delta = 16.2$, 121.4, 121.5, 122.3, 127.2, 127.3, 130.0, 131.4, 133.1, 135.8, 140.9, 142.7, 144.8, 191.9 ppm; HRMS (ESI+): *m/z* $[M+H]^+$ calcd for $C_{14}H_{11}OS_2$: 259.0173; found: 259.0110 & $[M+Na]^+$ calcd for $C_{14}H_{10}NaOS_2$: 281.0071; found: 280.9917.

[2-Methyl-4-(2-thienyl)benzo [*b*] thiophene-5-yl] methanol (32): 350 mg (1.35 mmol) of the aldehyde **31** on reduction with $NaBH_4$ (1.35 mmol) in ethanol for 2 hrs at r.t. and after usual work up, afforded the compound **32** as a yellowish oil. Yield: 320 mg (1.23 mmol, 91%); ^1H NMR (300 MHz, $CDCl_3$): $\delta = 2.13$ (br s, 1H), 2.49 & 2.54 (both s, total 3H), 4.59 & 4.68 (both s, total 2H), & 6.78 & 6.88 (both s, total 1H), 7.03 (d, $J = 2.4$ Hz, 1H), 7.11 & 7.12 (both d, $J = 3.6$ Hz, total 1H), 7.37 (d, $J = 8.4$ Hz, 1H), 7.39–7.41 (m, 1H), 7.71 (d, $J = 8.1$ Hz, 1H) ppm; NMR (400 MHz, $CDCl_3$): $\delta = 16.2$, 63.0, 121.5, 122.2, 123.8, 126.0, 127.1, 127.2, 127.8, 135.9, 138.7, 138.8, 141.3, 141.5 ppm; HRMS (ESI+): *m/z* $[M]^+$ calcd for $C_{14}H_{12}OS_2$: 260.0330; found: 260.1869.

2- [2-Methyl-4-(2-thienyl)benzo [*b*] thiophene-5-yl] acetonitrile (33): The compound **32** (310 mg, 1.19 mmol) was converted to the nitrile derivative **33** under the identical reaction condition, as used for the previous synthesis**,** asoff white solid; Yield: 270 mg (1 mmol, 84%); mp:106–108 °C; IR(KBr) ν_{max}: 2358 cm^{-1}; ^1H NMR (500 MHz, $CDCl_3$): $\delta = 2.53$ (s, 3H), 3.72 (s, 2H), 6.76 (s, 1H), 7.07 (d, $J = 3.0$ Hz,^1H), 7.19 (t, $J = 4.5$ Hz, 1H), 7.41 (d, $J = 8.5$ Hz, ^1H), 7.49 (d, $J = 5.0$ Hz, 1H), 7.79 (d, $J = 8.5$ Hz, ^1H) ppm; ^{13}C NMR (125 MHz, $CDCl_3$): $\delta = 16.3$, 22.1, 118.4, 121.5, 122.9, 123.8, 125.8, 126.8, 127.6, 128.2, 128.3, 138.2, 139.5, 142.0, 142.8 ppm; HRMS (ESI+): *m/z* $[M+Na]^+$ calcd for $C_{15}H_{11}NaNS_2$: 292.0231; found: 292.0236.

2- [2-Methyl-4-(2-thienyl)benzo [*b*] thiophen-5-yl] acetic acid (34): 260 mg (0.97 mmol) of the nitrile derivative **33** on hydrolysis with 4 ml 30% KOH in EtOH (reflux for 20 hrs) afforded the compound **34** as a white solid after usual work up and purification. Yield: 140 mg (0.49 mmol, 50%); mp: 170–172 °C; IR (KBr) ν_{max}: 1699 cm^{-1}; HRMS (ESI+): *m/z* $[M+Na]^+$ calcd for $C_{15}H_{12}O_2NaS_2$: 311.0176; found: 311.1094.

9-Methylnaptho [1,2-*b*:7,8-*b*′] bisthiophen-4-ol (35): Cyclization of the carboxylic acid **34** (120 mg, 0.42 mmol) with a mixture of 4.2 ml trifluoroacetic anhydride and 1.5 ml trifluoroacetic acid, afforded the compound **35** as a dark coloured semi solid mass, after usual work up and purification. Yield: 90 mg (0.33 mmol, 80%); ^1H NMR (500 MHz, $CDCl_3$): $\delta = 2.78$ (s, 3H), 5.47 (br s, 1H), 7.15 (s, 1H), 7.62 (d, $J = 5.0$ Hz, 1H), 7.65 (d, $J = 8.5$ Hz, 1H), 7.73 (d, $J = 5.5$ Hz, 1H), 7.82 (d, $J = 8.5$ Hz, 1H) 8.03 (s, 1H) ppm; ^{13}C NMR (125 MHz, $CDCl_3$): $\delta = 16.6$, 107.0, 120.3, 120.5, 120.8, 122.2, 123.0, 125.2, 130.3, 130.7, 136.3, 137.0, 141.2, 148.5, 211.40 ppm; HRMS (ESI+): *m/z* $[M+H]^+$ calcd for $C_{15}H_{11}OS_2$: 271.0173; found: 271.3785.

9-Methylnaphtho [1,2-*b*:7,8-*b*′] bisthiophen-4,5-dione (36): The phenolic compound **35** (80 mg, 0.3 mmol) on oxidation with 450 mg of Fremy's salt in 1/6 (M) Na_2HPO_4 solution (30 ml) and MeOH (12 ml) for overnight at 0–4 °C, afforded the o-quinone derivatives **36** as a deep violet solid, after usual work up and purification. Yield: 65 mg (0.23 mmol, 77%); mp: 227–228 °C; IR (KBr) ν_{max}: 1686 & 1657 cm^{-1}; ^1H NMR (400 MHz, $CDCl_3$ + DMSO-d_6): $\delta = 2.67$ (s, 3H), 7.53 (d, $J = 5.6$ Hz, 1H), 7.69 (d, $J = 5.6$ Hz, 1H), 7.87 (d, $J = 8.4$ Hz, 1H), 7.91 (d, $J = 8.4$ Hz, 1H), 8.14 (s, 1H) ppm; ^{13}C NMR (125 MHz, $CDCl_3$): $\delta = 21.6$, 125.8, 128.2, 129.1, 131.2, 131.9, 133.0, 139.7, 142.1, 151.1, 152.6, 178.9, 185.0 (2C short, sample was poorly soluble even in DMSO-d_6; possibly 2 quaternary carbons didn't appeared with this number of scanning) HRMS (ESI+): *m/z* $[M+H]^+$ calcd for $C_{15}H_9O_2S_2$: 284.9966; found: 284.8027 & $[M+Na]^+$ calcd for $C_{15}H_8O_2NaS_2$: 306.9863; found: 306.7510.

6,7-Dihydro-2-Methyl-4-(3-thienyl)-benzo [*b*] thiophene-5-carbaldehyde (37): 705 mg (2.71 mmol) the bromoaldehyde **29** was subjected to Suzuki coupling reaction with 3-thiopheneboronic acid (410 mg, 3.2 mmol) under the identical reaction condition, afforded the compound **37** after usual work up and purification as pale yellow solid; yield: 475 mg (1.82 mmol, 67%); mp: 55–56 °C; IR (KBr)ν_{max}: 1649 cm^{-1}; ^1H NMR (400 MHz, $CDCl_3$): $\delta = 2.31$ (s, 3H), 2.71–2.75 (m, 2H), 2.81–2.85 (m, 2H), 6.31 (s, 1H), 7.02 (dd, J = 1.2 & 4.8 Hz,1H), 7.24 (dd, ill split, J = 1.2 & 2.8 Hz, 1H), 7.35 (dd, J = 3.2 & 4.8 Hz, 1H), 9.59 (s, 1H) ppm; ^{13}C NMR (100 MHz, $CDCl_3$): $\delta = 15.2$, 21.5, 22.8, 124.0, 125.9, 126.4, 129.2, 130.6, 135.7, 136.0, 136.9, 141.5, 146.1, 192.6 ppm; HRMS (ESI+): *m/z* $[M+H]^+$ calcd for $C_{14}H_{13}OS_2$: 261.0330; found: 261.0750 & $[M+Na]^+$ calcd for $C_{14}H_{12}OS_2Na$: 283.0227; found: 283.689.

2-Methyl-4-(3-thienyl)benzo [*b*] thiophene-5-carbaldehyde (38): 420 mg (1.61 mmol) of compound **37** and 440 mg (1.94 mmol) of DDQ in 20 ml dry benzene was refluxed for 24 hrs protecting from moisture. After usual work up, the compound **38** was obtained as pale yellow solid.yield: 370 mg (1.43 mmol, 89%); mp: 102–103 °C; IR (KBr) ν_{max}: 1673 cm^{-1}; ^1H NMR (400 MHz, $CDCl_3$): $\delta = 2.56$ (s, 3H), 6.91 (s, 1H), 7.23 (dd, J = 0.8 & 4.8 Hz, 1H), 7.36 (dd, J = 2.8 & 4.8 Hz, 1H), 7.51 (dd, J = 2.8 & 4.8 Hz, 1H), 7.81 (d, $J = 8.4$ Hz, 1H), 7.90 (d, $J = 8.4$ Hz, 1H), 9.99 (s, 1H) ppm; ^{13}C NMR (100 MHz, $CDCl_3$): $\delta = 16.3$, 121.6, 121.7, 121.8, 125.9, 126.1, 130.0, 130.9, 136.1, 136.2, 140.5, 142.5, 145.2, 192.4 ppm; HRMS (ESI+): *m/z* $[M+H]^+$ calcd for $C_{14}H_{11}OS_2$: 259.0173; found: 259.0254.

[2-Methyl-4-(3-thienyl)benzo[*b*]thiophen-5-yl] methanol (39): 360 mg (1.39 mmol) of the aldehyde **38** on $NaBH_4$ (1.39 mmol) reduction in EtOH (2 hrs), afforded the compound **39** as colourless viscous liquid; yield: 340 mg (1.31 mmol, 94%); ^{1}H NMR (400 MHz, $CDCl_3$): $\delta = 2.34$ (s, 3H), 2.58 (br s, 1H), 4.33 (s, 2H), 6.59 (br s, 1H), 6.93 (dd, J = 1.2 & 4.8 Hz, 1H), 7.07 (dd, J = 1.2 & 3.2 Hz, 1H), 7.16 (d, $J = 8.0$ Hz, 1H), 7.21 (dd, J = 2.8 & 4.8 Hz, 1H), 7.48 (d, $J = 8.0$ Hz, 1H) ppm; ^{13}C NMR (100 MHz, $CDCl_3$): $\delta = 16.3$, 63.0, 121.5, 121.7, 123.9, 124.2, 125.4, 129.5, 130.2, 134.6, 138.6, 139.0, 140.5, 141.1 ppm; HRMS (ESI+): *m/z* $[M+Na]^+$ calcd for $C_{14}H_{12}OS_2Na$: 283.0227; found: 283.2804.

2-[2-Methyl-4-(3-thienyl)benzo[*b*]thiophen-5-yl] acetonitrile (40): The alcohol **39** (310 mg, 1.19 mmol) was converted to the cyanide **40** (under the identical reaction condition), as a pale yellow low melting solid; yield: 285 mg (1.06 mmol, 89%); IR (KBr) ν_{max}: 2242 cm^{-1}; ^{1}H NMR (400 MHz, $CDCl_3$): $\delta = 2.45$ (s, 3H), 4.54 (s, 2H), 6.67 (s, 1H), 7.10 (dd, J = 1.4 & 5.2 Hz, 1H), 7.27 (dd, J = 1.4 & 2.4 Hz, 1H), 7.34 (d, $J =$ 8.4 Hz, 1H), 7.38 (dd, J = 2.4 & 5.2 Hz, 1H), 7.67 (d, $J = 8.0$ Hz, 1H) ppm; ^{13}C NMR (100 MHz, $CDCl_3$): $\delta = 16.2$, 121.5, 123.9, 124.1, 125.4, 129.4, 130.4, 134.6, 138.5, 139.1, 140.6, 141.2 (3C Short, possibly three quaternary carbons didn't appeared with this number of scanning) ppm; HRMS (ESI+): *m/z* $[M+Na]^+$ calcd for $C_{15}H_{11}NS_2Na$: 292.0231; found: 292.0465.

2-[2-Methyl-4-(3-thienyl)benzo[*b*]thiophen-5-yl] acetic acid (41): 260 mg (0.97 mmol) of the nitrile derivative **40** on hydrolysis with 4 ml 30% KOH in EtOH under reflux for 20 hrs, afforded the compound **41** as a white solid after usual work up and purification. Yield: 160 mg (0.56 mmol, 58%); IR (KBr) ν_{max}: 1697 cm^{-1}; HRMS (ESI+): *m/z* $[M+H]^+$ calcd for $C_{15}H_{13}O_2S_2$: 289.0357; found: 289.0103 & *m/z* $[M+Na]^+$ calcd for $C_{15}H_{12}O_2S_2Na$: 311.0176; found: 310.9653.

9-Methylnaphtho[2,1-*b*:7,8-*b*′]bisthiophen-4-ol (42): Cyclization of the carboxylic acid **41** (120 mg, 0.42 mmol) with a mixture of 4 ml trifluoroacetic anhydride and 1.5 ml trifluoroacetic acid under the identical reaction condition, afforded the compound **42** as a reddish semi solid mass, after usual work up and purification. yield: 105 mg (0.39 mmol, 93%); ^{1}H NMR (500 MHz, $CDCl_3$): $\delta = 2.76$ (s, 3H), 5.66 (br s, 1H), 7.18 (s, 1H), 7.65 (d, $J = 8.5$ Hz, 1H), 7.72 (d, $J = 5.5$ Hz, 1H), 7.82 (d, $J = 8.5$ Hz, 1H), 8.00 (s, 1H), 8.4 (d, $J = 5.0$ Hz, 1H) ppm; ^{13}C NMR (125 MHz, $CDCl_3$): $\delta =$ 29.8, 95.9, 105.5, 107.0, 108.3, 120.6, 122.4, 125.3, 126.3, 129.4, 131.5, 193.9 (three Carbon short, possibly three quaternary carbons didn't appeared with this number of scanning) ppm; HRMS (ESI+): *m/z* $[M+H]^+$ calcd for $C_{15}H_{11}OS_2$: 271.0173; found: 270.9474.

9-Methylnaphtho[2,1-*b*:7,8-*b*′]bisthiophene-4,5-dione (43): Oxidation of the phenolic compound **42** (80 mg, 0.3 mmol) with 450 mg (1.68 mmol) of Fremy's salt, under the identical reaction condition, afforded the compound **43** as a deep red solid, after usual work up and purification. yield: 70 mg (0.25 mmol, 83%); mp: 230–232 °C; IR (KBr) ν_{max}: broad strong peak at 1652 cm^{-1}; ^{1}H NMR (500 MHz, $CDCl_3$): $\delta =$ 2.61 (s, 3H), 7.47 (s, 1H), 7.68 (d, $J = 8.4$ Hz, 1H), 7.81 (d, $J = 5.2$ Hz, 1H), 7.84 (d, $J = 5.2$ Hz, 1H), 7.96 (d, $J = 8.4$ Hz, 1H) ppm; HRMS (ESI+): *m/z* $[M+H]^+$ calcd for $C_{15}H_9O_2S_2$: 284.9966; found: 285.1825 & $[M+Na]^+$ calcd for $C_{15}H_8O_2S_2Na$: 306.9863; found: 307.1755.

Methyl 2-[2-(2-thienyl)phenyl] acetate (45): A stirred mixture of 500 mg (2.18 mmol) of bromo ester **44,** 2-thiopheneboronic acid (2.62 mmol), triethylamine (5.45 mmol) in 4 ml of DMF was degasified for 25 min by bubbling N_2 through it. Now to it, $Pd(PPh_3)_4$ catalyst (2 mol%) was added quickly and degasified for another 15 min. The mixture was then heated at about 110 °C for 6 hrs under N_2 atmosphere. When the reaction was completed (checked by TLC), the mixture was poured into ice water (15–20 ml) and extracted thoroughly with ether (3 × 20 ml). Organic layer was washed with ice water, 5% aq. $NaHCO_3$ solution and finally with ice water. Removal of solvent afforded the crude product which on purification by column chromatography [silica gel 100–200 mesh / P.E (60–80 °C)-EtOAc, 15:1] furnished the compound **45** as a yellow oil. Yield: 330 mg, 65%. IR (KBr) ν_{max}: 1738 cm^{-1}; ^{1}H NMR (400 MHz, $CDCl_3$): δ 3.57 (s, 3H), 3.67 (s, 2H), 6.96–7.01(m, 2H), 7.21–7.26 (m, 4H), 7.34 (dd, $J = 2$ Hz and 8.0 Hz, 1H) ppm;^{13}C NMR (100 MHz, $CDCl_3$): $\delta = 39.1$, 52.0, 125.7, 127.0, 127.2, 127.2, 128.2, 130.7, 131.2, 132.7, 134.7, 141.9, 172.2 ppm; HRMS (ESI+): *m/z* $[M+Na]^+$ calcd for $C_{13}H_{12}O_2SNa$: 255.0456; found: 254.8899.

2-[2-(2-Thienyl)phenyl] acetic acid (46): To a solution of the compound **45** (310 mg, 1.34 mmol) in ethanol (3 ml), 4 ml 30% aq. KOH solution was added. It was refluxed for 12 hrs. Excess ethanol was removed by distillation and the residue was diluted with ice-water (5 ml). It was extracted with ether (2 × 15 ml).The aqueous part was acidified with 1:1 HCl under ice-cold condition. The precipitated acid was filtered and washed thoroughly with cold water and dried. The crude acid **46** thus obtained was re-dissolved in saturated aq. $NaHCO_3$ solution, filtered to remove any suspended impurities. The filtrate was cooled in ice bath was acidified 1:1 aq. HCl. The acid **46** precipitated as white solid was filtered and dried to furnish the title compound **46** as off white solid. Yield: 240 mg, 78%. M.P: 185–186 °C. IR (KBr) ν_{max}: 1693 cm^{-1}; HRMS (ESI+): *m/z* $[M+Na]^+$ calcd for $C_{12}H_{10}O_2SNa$: 241.0299; found: 241.1128.

Naphtho[1,2-*b*]thiophene-4-ol (47): To an ice cold magnetically stirred mixture of 230 mg (1 mmol) of the acid **46** and 9 ml of trifluoroacetic anhydride, 2.5 ml trifluoroacetic acid was injected slowly at 0–4 °C and stirred further for 1 hr protecting from moisture and then left in the refrigerator for overnight. The reaction mixture was decomposed with crushed ice and extracted with dichloromethane thoroughly. The organic layer was washed with cold aq. $NaHCO_3$ solution, cold brine solution and dried (anhyd. Na_2SO_4). Removal of the solvent and purification of the crude product by plate chromatography (Silica gel GF254; benzene), the phenol **47** was obtained as semi solid mass. Yield: 160 mg (0.8 mmol, 80%); ^{1}H NMR (400 MHz, $CDCl_3$): $\delta = 5.48$ (br s, 1H), 7.01 (s, 1H), 7.43–7.46 (m, 2H), 7.51 (d, $J = 5.4$ Hz, 1H), 7.63 (d, $J = 5.4$ Hz, 1H), 7.76 (d, $J = 7.4$ Hz, 1H), 8.06 (d, $J = 7.4$ Hz, 1H) ppm; ^{13}C NMR (100 MHz, $CDCl_3$): $\delta = 105.4$, 122.6, 123.2, 123.7, 124.2, 124.5, 125.9, 126.5, 127.0, 127.4, 134.4, 148.7 ppm; HRMS (ESI+): *m/z* $[M+H]^+$ calcd for $C_{12}H_9OS$: 201.0296; found: 201.0602.

Naphtho[1,2-*b*]thiophene-4,5-dione (48): To a vigorously stirred solution of 900 mg Fremy's salt in 20 ml aq. 1/6M disodium hydrogen phosphate at 0–5 °C, a solution of the phenol **47** (130 mg, 0.65 mmol) in MeOH (8 ml) was added drop wise. The colour of the solution quickly changes from violet to reddish brown with formation of dark red to deep red ppt. Stirring was continued at 0–5 °C for an additional hour and the mixture was left in the refrigerator for overnight. The reaction mixture was then extracted with dichloromethane, washed with cold water, dried (anhyd. Na_2SO_4) and solvent removed. Crude *o*-quinone derivative thus obtained on further purification by preparative TLC (Silica gel GF254 mesh; benzene-methanol, 5:1) followed by recrystallisation from MeOH afforded the title compound **48** as deep orange solid. Yields: 100 mg (0.47 mmol), 72%; mp: 207–208 °C. IR (KBr) ν_{max}: br peak 1659 cm^{-1}. ^{1}H NMR (400 MHz, $CDCl_3$): $\delta = 7.19$ (d, $J = 5.2$ Hz, 1H), 7.34 (ddd, J = 0.8, 7.6 & 7.6 Hz, 1H), 7.45 (d, $J = 7.6$ Hz, 1H), 7.46 (d, $J =$ 5.2 Hz, 1H), 7.53 (ddd, J = 1.6, 7.6 & 7.6 Hz, 1H), 8.00 (d, J = 0.8 and 7.2 Hz, 1H) ppm; ^{13}C NMR (100 MHz, $CDCl_3$): $\delta = 124.7$, 126.0, 127.8, 129.1, 129.7, 130.2, 132.4, 135.8, 136.5, 151.2, 173.8, 180.4 ppm; HRMS (ESI+): *m/z* $[M+H]^+$ calcd for $C_{12}H_7O_2S$: 215.0089; found: 214.9340 and $[M+Na]^+$ calcd for $C_{12}H_6O_2SNa$: 236.9986; found: 236.9225.

Methyl 2-[2-(3-thienyl)phenyl] acetate (49): 500 mg (2.18 mmol) of the bromoester **44** was subjected to Suzuki coupling reaction with 3-thiopheneboronic acid (2.62 mmol) under the identical reaction condition, as used for the preparation of the compound **45,** and 365 mg (1.57 mmol, 72%) of the compound **49** (yellowish oil) was obtained after usual work up and purification. IR (KBr) ν_{max}: 1727 cm^{-1}. ^{1}H NMR (400 MHz, $CDCl_3$): $\delta = 3.55$ (s, 3H), 3.57 (s, 2H), 7.03 (dd, J = 1.6 and 4.8 Hz, 1H), 7.17 (dd, J = 1.6 and 3.2 Hz, 1H), 7.21–7.27 (m, 5H) ppm; ^{13}C NMR (100 MHz, $CDCl_3$): $\delta = 38.9$, 52.0, 123.2, 125.4, 127.2, 127.6, 129.0, 130.3, 130.5, 132.1, 137.2, 141.2, 172.4 ppm. HRMS (ESI+): *m/z*

$[M+Na]^+$ calcd for $C_{13}H_{12}O_2SNa$: 255.0456; found: 254.8899.

2-[2-(3-Thienyl)phenyl] acetic acid (50): 340 mg (1.47 mmol) of the ester **49** on hydrolysis with 4 ml ethanolic 30% KOH, under the identical reaction condition, as used for the preparation of the compound **46** afforded the compound **50** as a white solid, after usual work up and purification. Light brown solid. Yield: 280 mg (1.22 mmol, 83%); mp: 188–190 °C. IR (KBr) ν_{max}: 1699 cm^{-1}; HRMS (ESI+): *m/z* $[M+Na]^+$ calcd for $C_{12}H_{10}O_2SNa$: 241.0299; found: 241.1128.

Naphtho[2,1-*b*]thiophene-4-ol (51): Cyclization of the carboxylic acid **50** (260 mg, 1.13 mmol) with the mixture of 7 ml trifluoroacetic anhydride and 3 ml trifluoroacetic acid, under the identical reaction condition, as used for the preparation of the compound **47** afforded after usual work up the compound **46** and purification of it the phenol **51** was obtained as a brown low melting solid. Yield: 170 mg (0.85 mmol, 52%). ^1H NMR (400 MHz, $CDCl_3$): $\delta = 6.89$ (br s, 1H), 7.17 (s, 1H), 7.41(d, $J =$ 5.2 Hz,1H), 7.43–7.48 (m, 2H), 7.64 (d, $J = 5.2$ Hz, 1H), 7.91 (d, $J = 7.6$ Hz, 1H), 7.95 (d, $J = 7.6$ Hz, 1H) ppm; ^{13}C NMR (100 MHz, $CDCl_3$): $\delta =$ 105.4, 108.4, 121.2, 123.4, 124.2, 124.3, 125.8, 125.9, 127.5, 129.4, 148.6, 162.6 ppm; HRMS (ESI+): *m/z* $[M+H]^+$ calcd for $C_{12}H_9OS$: 201.0296; found: 201.0256.

Naphtho[2,1-*b*]thiophene-4,5-dione (52): The phenolic compound **51** (130 mg, 0.65 mmol) on oxidation with 900 mg of Fremy's salt under the identical reaction condition, as used for the preparation of the compound **47,** afforded the *o*-quinone **52** as a deep yellow solid, after usual work up and purification. Yield: 120 mg (0.56 mmol, 86%). Mp: 210–212 °C. IR (KBr) ν_{max}: 1634 and 1651 cm^{-1}. ^1H NMR (400 MHz, $CDCl_3$): $\delta = 7.34$–7.38 (m,1H), 7.45 (d, $J = 4.8$ Hz 1H), 7.56–7.60 (m, 2H), 7.79 (d, $J = 5.2$ Hz, 1H), 8.03 (dd, J = 0.8 and 7.6 Hz, 1H) ppm; ^{13}C NMR (100 MHz, $CDCl_3$): $\delta =$ 124.5, 125.1, 129.7, 130.0, 130.8, 133.0, 135.8, 138.7, 146.7, 172.5, 180.9 ppm (one quarternary carbon was not observed possibly due to insufficient number of scanning); HRMS (ESI+): *m/z* $[M+H]^+$ calcd for $C_{12}H_7O_2S$: 215.0089; found: 215.1627 and $[M+Na]^+$ calcd for $C_{12}H_6O_2SNa$: 236.9986; found: 237.1626.

Drugs, antibodies and plasmids: Tanshinone I (T5330), Tanshinone IIA (T4952) and Chloroquine diphosphate salt (C6628) were purchased from Sigma-Aldrich Corp. (St. Louis, MO, USA).

Mouse monoclonal antibodies directed against p62/SQSTM1 (Clone# 3/*P*62 lck ligand), Beclin1 (Clone# 20/Beclin) and cleaved PARP (Clone# Asp214) were purchased from BD Biosciences (Franklin Lakes, NJ, USA). Rabbit monoclonal antibody directed against Bcl-2 (D55G8), Bcl-xL (54H6), Bax (D2E11), Bim (C34C5), Bak1 (D4E4) and mouse monoclonal antibody against CHOP (L63F7) were purchased from Cell Signaling Technology Inc. (Danvers, MA). Mouse monoclonal antibodies against GAPDH (0411), p53 (DO-1), MAPLC3B (G-9), ATF4 (C-20) and GADD34 (D8) were purchased from Santa Cruz Biotechnology (Santa Cruz, CA, USA). DyLight 800/680 conjugated (for western blots) and Alexa Fluor 488/555 tagged (for confocal micoscopy) secondary antibodies anti-mouse, anti-rabbit, anti-sheep IgG (H + L) were purchased from Thermo Fisher Scientific Inc. (Waltham, MA, USA).

pBabePuro-GFP-LC3 construct expressing GFP-tagged LC3B was a kind gift from Jayanta Debnath (Addgene plasmid# 22405) and mCherry-tagged p62 plasmid expressing plasmid was generously provided by Edward M. Campbell (Loyola University Chicago, IL, USA)

Cell lines and Cell culture: Human breast cancer MCF7 (ER^+ PR^+ $Her2^-$) cells were obtained from Gaurisankar Sa (Bose Institute, Kolkata) and MDA-MB-231 (ER^- PR^- $Her2^-$) were obtained from Ranjana Pal (Presidency University, Kolkata). MCF7 and MDA-MB-231 cell lines were maintained in Dulbecco's modified Eagle's medium (DMEM) (Gibco, Invitrogen, Thermo Fisher Scientific Inc.) and Roswell Park Memorial Institute medium (RPMI) (Gibco, Invitrogen, Thermo Fisher Scientific Inc.), respectively at 37 °C in a humidified environment that contains 5% CO_2. The culture medium was supplemented with 10% FBS (Fetal Bovine Serum; Gibco/Invitrogen, Inc., USA) and 1% penicillin-streptomycin solution (Sigma-Aldrich Corp., St. Louis, MO).

Cytotoxicity assay by MTT: Cell viability was measured using MTT (Sigma-Aldrich Corp., St. Louis, MO) as per manufacturer's instructions. Briefly, $\sim 5 \times 10^3$ MCF7 or MDA-MB-231 cells seeded in a 96 well plate were treated with drugs in increasing concentrations (0–40 μM). 24 h post-treatment MTT was added at a concentration of 0.5 mg/ml and after 3 h the media was discarded and 200 μL of DMSO was added in each well to dissolve the insoluble purple formazan crystals. The absorbance was measured at 540 nm using a microplate reader (Synergy H1; Bio Tek) and subsequently IC_{50} of respective compounds were calculated from plotted graphs. Experiments were performed in duplicate and were independently repeated two times.

Cell morphology analysis: $\sim 5 \times 10^4$ MCF7 or MDA-MB-231 cells plated in 6 well plates were either left untreated (DMSO control) or treated with 2.5 μM drugs. The morphological changes and characteristics for cell death were captured using Fluorescence cell imager (BIO-RAD, Hercules, CA, USA) at different time intervals (0, 6, 12 and 24 h).

Apoptosis assay by EtBr/AO staining: $\sim 5 \times 10^4$ MCF7 cells plated in 6-well plates with a coverslip inside in each well were either left untreated (DMSO control) or treated with 2.5 μM two natural tanshinones (compounds **1** and **2**) along with compounds **27**, **48** and **52**. 24 h post-treatment the media was discarded, washed with PBS and subsequently stained with 1:1 solution of ethidium bromide (EtBr) and acridine orange (AO) (0.4 mg/ml each). The cells were then immediately washed with 1 × PBS and mounted on a slide using Fluoromount (Invitrogen, Thermo Fisher Scientific Inc.). Apoptosis was assessed by identifying apoptotic, viable and nonviable cells using a Carl Zeiss Fluorescence microscope with an Apotome.2 attachment (Carl Zeiss AG, Germany) with a blue excitation (480 nm) and a barrier filter (515–530 nm). Typically, AO stains viable cells as green, while EtBr stains the nucleus as red (bright orange) in response to apoptotic induction. The apoptosis and cell viability assessments were performed based on 200 cells per sample and represented as bar diagrams.

Apoptosis assay by annexin V/PI staining: Cell apoptosis induced by tanshinones and the three derivatives – compounds **27**, **48** and **52** was determined by Annexin V-FITC Apoptosis Staining/Detection Kit (ab14085) according to manufacturer's protocol (Abcam Cambridge, UK). Briefly, $\sim 5 \times 10^5$ MCF7 or MDA-MB-231 cells were either left untreated (DMSO control) or treated with different tanshinone analogues. 24 h post-treatment cells were collected by centrifugation and re-suspended in 500 μL of 1X binding buffer. Next, cells were stained with 5 μL of Annexin V-FITC and 5 μL of propidium iodide (PI) (Sigma-Aldrich Corp. St. Louis, MO, USA) for 5 min at room temperature in the dark. FITC labelled Annexin V binding (Ex = 488 nm; Em = 350 nm) and PI staining were detected using FITC signal detector by the phycoerythrin emission signal detector in BD Accuri C6 Flow Cytometry Analyzer (BD Biosciences, San Jose, CA, USA). Experiments were performed in duplicate and presented the data as an average with SE+/−.

Western blot analysis: $\sim 10 \times 10^6$ MCF7 or MDA-MB-231 cells were either left untreated (DMSO control) or treated with 2.5 μM tanshinone analogues. 24 h post-treatment, cells were harvested, washed with ice cold 1X PBS (Gibco/Invitrogen, Inc., USA), and subsequently lysed in 0.5 ml ice cold RIPA buffer (Sigma-Aldrich Corp., St. Louis, MO) with protease inhibitor (Cell Signalling Technology Inc., Danvers, MA, USA). Protein samples were estimated by Bradford reagent (BIO-RAD, Hercules, CA, USA). Samples were boiled in laemmeli buffer (BIO-RAD, Hercules, CA), fractionated by SDS-PAGE and transferred to a 0.45 μm nitrocellulose membrane (BIO-RAD, Hercules, CA). The membranes were then probed with specific antibodies incubated overnight at 4 °C followed by incubation with appropriate infrared-tagged/DyLight secondary antibodies for 1 h at 37 °C and viewed on an Odyssey CLx Imaging System (LiCor Inc., Lincoln, NE, USA). Image analysis and quantification measurements were performed using the Odyssey Infrared Imaging System application software (LiCor Inc., Lincoln, NE, USA).

RNA extraction and real-time PCR analysis: Total RNA was isolated from $\sim 10 \times 10^6$ MCF7 or MDA-MB-231 cells either left untreated (DMSO control) or treated with 2.5 μM tanshinone analogues for 24 h using TRIzol reagent according to the manufacturer's instructions

(Invitrogen, Thermo Fisher Scientific Inc., Waltham, MA, USA), followed by cDNA preparation using iScript cDNA synthesis kit (BIO-RAD, Hercules, CA, USA) as per manufacturer's protocol. RNA and cDNA quality and quantity were checked using Synergy H1 Multimode Microplate Reader (BioTek Instruments, Inc., VT, USA). qPCR analysis was performed using iTaq Universal SYBR Green Supermix (BIO-RAD, Hercules, CA, USA) in CFX Connect™ Real-Time PCR detection System (BIO-RAD, Hercules, CA, USA) with the following thermal profile – 1 cycle: 95 °C for 10 min; 40 cycles: 95 °C for 15 *sec* followed by 60 °C for 1 min; and finally the dissociation curve at – 95 °C for 1 min, 55 °C 30 min, and 95 °C for 30 *sec*. Unless and otherwise stated, each sample was performed in duplicate and calculation was made using a $2^{-\Delta\Delta CT}$ method to quantify relative expression compared with housekeeping gene control. The real time PCR primers used in this study were designed from Primer-BLAST (https://www.ncbi.nlm.nih.gov/tools/primer-blast/) and listed in **Table S2**. Real-time PCR primers were obtained from Integrated DNA Technologies, Inc. (Coralville, IA, USA).

Transfection: For confocal microscopy, ~10×10^5 MCF7 cells were transiently transfected with plasmids expressing GFP-tagged LC3 or mCherry-tagged p62 using Lipofectamine 3000 according to manufacturer's protocol (Invitrogen, Thermo Fisher Scientific Inc., Waltham, MA, USA). 24 h post-transfection cells were either left untreated or treated with natural tanshinones or different synthetic compounds for another 24 h and subjected to live-cell confocal microscopy analyses.

Confocal microscopy: For live cell imaging, ~1×10^6 MCF7 cells grown at 70% confluency on 35 mm dish embedded with 12 mm glass viewing area (Nunc, Thermo Fisher Scientific Inc., Waltham, MA, USA) were transfected with GFP-LC3 or mCherry-p62 expressing constructs as described above. 24 h post-transfection, cells were either left untreated (DMSO control) or treated with 2.5 μM drugs for another 24 h. Hoechst 3342 solution (Thermo Fisher Scientific Inc., Waltham, MA, USA) and LysoTracker Red DND-99 (Invitrogen, Thermo Fisher Scientific Inc., Waltham, MA, USA) were used to stain the nucleus and the acidic lysosomes, respectively. The images were obtained by a Leica DMi8 Confocal Laser Scanning Microscope and analyzed in the Leica Application Suite X (LAS X) software (Leica Microsystems GmbH, Wetzlar, Germany).

PCR microarray: To identify the transcriptional deregulation of unfolded protein response (UPR) genes in response to drug treatment, a 96-well set-up for 'Unfolded Protein Response RT2 Profiler PCR Array' (SABiosciences, Frederick, MD, USA) was performed using ~10×10^6 MCF7 cells either left untreated (DMSO control) or treated with 2.5 μM compounds **48** and **52** for 24 h. ~1 μg of amplified cDNA of each sample was subjected to PCR microarray analyses according to the manufacturer's instructions. Real-time PCR was performed was performed using SsoFast EvaGreen Supermix (BIO-RAD, Hercules, CA, USA) in CFX Connect™ Real-Time PCR detection System under the same conditions as described above. Data analysis is based on the $2^{-\Delta\Delta Ct}$ method with normalization of the raw data to the DMSO control sample and represented as heat map analyses (log_2). Data analysis was carried out using an algorithm provided at manufacturer's web portal. Each array contained 5 housekeeping genes (HKGs) - ACTB, B2M, GAPDH, HPRT1 and RPLP0. The average ΔCt value of HKGs was used to normalize the sample data. Any Ct value greater than 35 of total 84-key genes was not accounted in calculation. If the Ct value of the human genomic DNA control (HGDC) was greater than 30, it indicated RNA was free of any genomic DNA contamination. The statistical analysis was performed based on the calculation of p-values using a Student's *t*-test. The 84 autophagy related genes of the profiler array are listed in **Table S3**.

Statistical analysis: All the data represented are as the mean values with standard errors of means (SEM). Statistical significance of differences in the mean values was analyzed using the Student's *t*-test two tail distribution and equal variances between two samples. P-value below 0.05 was considered as significant (*$P < 0.05$; **$P < 0.01$; ***$P < 0.001$; ns, not significant).

Declaration of Competing Interest

The authors declare that they have no known competing financial interests or personal relationships that could have appeared to influence the work reported in this paper.

Acknowledgements

We sincerely thank to Jayanta Debnath (University of California, San Francisco, USA), Edward M. Campbell (Loyola University Chicago, IL, USA), Gaurisankar Sa (Bose Institute, Kolkata, India) and Ranjana Pal (Presidency University, Kolkata, India) for providing reagents, plasmids and cell lines. We also thank Pralay Majumder (Presidency University, Kolkata, India) for technical support in using Microscopy Facility at Dept. Life Sciences, Presidency University, Kolkata, India. A.S. is a Wellcome Trust/DBT India Alliance Intermediate Fellow. C.G. is the recipient of UGC-NET Senior Research Fellowship, India.

Financial Disclosure

This work was supported by grants from Wellcome Trust/DBT India Alliance Intermediate Fellowship research grant (IA/I/14/2/501537), Department of Biotechnology (DBT), Govt. of India (BT/PR8123/MED/30/990/2013) and Department of Science and Technology (DST), Govt. of India (CRG/2018/001044) to AS and Department of Science and Technology (DST), Govt. of India (SR/S1/OC-30/2011) to GKK. The funders had no role in study design, data collection and analysis, decision to publish, or preparation of the manuscript.

Appendix A. Supplementary material

Supplementary data to this article can be found online at https://doi.org/10.1016/j.bmc.2021.116112.

References

[1] Chen W, Chen G. Danshen (Salvia miltiorrhiza Bunge): A Prospective Healing Sage for Cardiovascular Diseases. Curr Pharm Des 2017;23:5125–35. CPD-EPUB-85406 [pii]10.2174/1381612823666170822101112.

[2] Li MH, Chen JM, Peng Y, Wu Q, Xiao PG. Investigation of Danshen and related medicinal plants in China. J Ethnopharmacol 2008;120:419–26. S0378-8741(08)00505-9 [pii]10.1016/j.jep.2008.09.013.

[3] Chen X, Guo J, Bao J, Lu J, Wang Y. The anticancer properties of Salvia miltiorrhiza Bunge (Danshen): a systematic review. *Med Res Rev*. Jul 2014;34:768–794. https://doi.org/10.1002/med.21304.

[4] Zhou L, Zuo Z, Chow MS. Danshen: an overview of its chemistry, pharmacology, pharmacokinetics, and clinical use. J Clin Pharmacol 2005;45:1345–59. 45/12/1345 [pii]10.1177/0091270005282630.

[5] Sarkar A, Das R, Kar GK. Thiophene Analogue of Isotanshinone-II Nucleus: A Novel Approach towards the Synthesis of Phenanthro[4,3-b]-thiophene-4,5-dione and Phenanthro[3,4-b]-thiophene-4,5-dione Derivatives. *Chem Select*. 2018;3:11422–11426. https://doi.org/10.1002/slct.201802652.

[6] Gao H, Huang L, Ding F, et al. Simultaneous purification of dihydrotanshinone, tanshinone I, cryptotanshinone, and tanshinone IIA from Salvia miltiorrhiza and their anti-inflammatory activities investigation. Sci Rep. 2018;8:8460. 10.1038/s41598-018-26828-010.1038/s41598-018-26828-0 [pii].

[7] Ma K, Zhang C, Huang MY, Guo YX, Hu GQ. Crosstalk between Beclin-1-dependent autophagy and caspasedependent apoptosis induced by tanshinone IIA in human osteosarcoma MG-63 cells. *Oncol Rep*. Oct 2016;36:1807–1818. https://doi.org/10.3892/or.2016.5003.

[8] Lv C, Zeng HW, Wang JX, et al. The antitumor natural product tanshinone IIA inhibits protein kinase C and acts synergistically with 17-AAG. Cell Death Dis 2018;9:165. 10.1038/s41419-017-0247-510.1038/s41419-017-0247-5 [pii].

[9] Wang X, Wei Y, Yuan S, et al. Potential anticancer activity of tanshinone IIA against human breast cancer. *Int J Cancer*. 2005;116:799–807. https://doi.org/10.1002/ijc.20880.

[10] Ding C, Tian Q, Li J, et al. Structural Modification of Natural Product Tanshinone I Leading to Discovery of Novel Nitrogen-Enriched Derivatives with Enhanced Anticancer Profile and Improved Drug-like Properties. *J Med Chem*. 2018;61:760–776. https://doi.org/10.1021/acs.jmedchem.7b01259.

[11] Liu W, Zhou J, Geng G, Shi Q, Sauriol F, Wu JH. Antiandrogenic, maspin induction, and antiprostate cancer activities of tanshinone IIA and its novel derivatives with modification in ring A. *J Med Chem*. 2012;55:971–975. https://doi.org/10.1021/jm2015292.

[12] Munagala R, Aqil F, Jeyabalan J, Gupta RC. Tanshinone IIA inhibits viral oncogene expression leading to apoptosis and inhibition of cervical cancer. Cancer Lett 2015; 356:536–46. S0304-3835(14)00578-3 [pii]10.1016/j.canlet.2014.09.037.

[13] Yu J, Wang X, Li Y, Tang B. Tanshinone IIA suppresses gastric cancer cell proliferation and migration by downregulation of FOXM1. *Oncol Rep*. Mar 2017;37: 1394–1400. https://doi.org/10.3892/or.2017.5408.

[14] Liao X, Gao Y, Liu J, et al. Combination of Tanshinone IIA and Cisplatin Inhibits Esophageal Cancer by Downregulating NF-kappaB/COX-2/VEGF Pathway. *Front Oncol*. 2020;10:1756. https://doi.org/10.3389/fonc.2020.01756.

[15] Chiu CM, Huang SY, Chang SF, Liao KF, Chiu SC. Synergistic antitumor effects of tanshinone IIA and sorafenib or its derivative SC-1 in hepatocellular carcinoma cells. *Onco Targets Ther*. 2018;11:1777–1785. https://doi.org/10.2147/OTT.S161534ott-11-1777 [pii].

[16] Lee CY, Sher HF, Chen HW, et al. Anticancer effects of tanshinone I in human non-small cell lung cancer. Mol Cancer Ther 2008;7:3527–38. 7/11/3527 [pii] 10.1158/1535-7163.MCT-07-2288.

[17] Li M, Gao F, Zhao Q, Zuo H, Liu W, Li W. Tanshinone IIA inhibits oral squamous cell carcinoma via reducing Akt-c-Myc signaling-mediated aerobic glycolysis. Cell Death Dis 2020;11:381. 10.1038/s41419-020-2579-910.1038/s41419-020-2579-9 [pii].

[18] Li N, Yang L, Zhang B, Chen S. Tanshinone IIA effects on ovarian cancer cell line. *J Pharm Pharmacol*. Oct 2018;70(10):1369–1377. https://doi.org/10.1111/jphp.12961.

[19] Wang J, Wang X, Jiang S, et al. Growth inhibition and induction of apoptosis and differentiation of tanshinone IIA in human glioma cells. *J Neurooncol*. Mar 2007;82: 11–21. https://doi.org/10.1007/s11060-006-9242-x.

[20] Wu Q, Zheng K, Huang X, Li L, Mei W. Tanshinone-IIA-Based Analogues of Imidazole Alkaloid Act as Potent Inhibitors To Block Breast Cancer Invasion and Metastasis in Vivo. *J Med Chem*. 2018;61:10488–10501. https://doi.org/10.1021/acs.jmedchem.8b01018.

[21] Shah R, Verma PK. Therapeutic importance of synthetic thiophene. Chem Cent J 2018;12:137. 10.1186/s13065-018-0511-510.1186/s13065-018-0511-5 [pii].

[22] Archna, Pathania S, Chawla PA. Thiophene-based derivatives as anticancer agents: An overview on decade's work. Bioorg Chem 2020;101:104026. S0045-2068(20) 31323-7 [pii].

[23] Samanta K, Kar GK, Sarkar AK. A generalised route for the synthesis of β-furyl-α, β-unsaturated aldehydes through Suzuki reactions. *Tetrahedron Lett*. 2008;49: 1461–1464.

[24] Shaik FH, Kar GK. Studies on polynuclear furoquinones. Part 1: Synthesis of tri- and tetra-cyclic furoquinones simulating BCD/ABCD ring system of furoquinone diterpenoids. *Beilstein J Org Chem*. 2009;5:1–7. https://doi.org/10.3762/bjoc.5.47.

[25] Sarkar A, Das R, Kar GK. A Suzuki-Coupling-Based Generalized Route for the Synthesis of 2-(2/3-Thienyl)cycloalk-1-ene-1-carbaldehydes as Precursors for Condensed Thienophenanthraquinones. *Synlett*. 2018;29:344–348.

[26] Mishra R, Kumar N, Mishra I, Sachan N. A Review on Anticancer Activities of Thiophene and its Analogs. Mini Rev Med Chem 2020;MRMC-EPUB-108183 [pii] 10.2174/1389557520666200715104555.

[27] Shah R, Verma PK. Synthesis of thiophene derivatives and their anti-microbial, antioxidant, anticorrosion and anticancer activity. *BMC Chem*. Dec 2019;13:54. https://doi.org/10.1186/s13065-019-0569-8569 [pii].

[28] Buu-Hoi NP, Hoan N, Khoi NH. Thiophene series. IV Thiophenocarbazoles, thiophenobenzocarbazoles, and their isocyclic analogs, and thiophenoacridines. *Recl Trav Chim Pays-Bas*. 1950;69:1053–1079.

[29] Acuna J, Piermattey J, Caro D, et al. Synthesis, Anti-Proliferative Activity Evaluation and 3D-QSAR Study of Naphthoquinone Derivatives as Potential Anti-Colorectal Cancer Agents. Molecules 2018;23.molecules23010186 [pii]10.3390/molecules23010186.

[30] Pereyra CE, Dantas RF, Ferreira SB, Gomes LP, Silva-Jr FP. The diverse mechanisms and anticancer potential of naphthoquinones. *Cancer Cell Int*. 2019;19:207. https://doi.org/10.1186/s12935-019-0925-8925 [pii].

[31] Lee J, Snyder JK. Ultrasound-promoted cycloadditions in the synthesis of Salvia miltiorrhiza abietanoid o-quinones. *J Org Chem*. 1990;55:4995–5008.

[32] Brandao AFM, de Oliveira AB, Snieckus V. Combined directed metalation - cross coupling strategies. A regiospecific route to heteroring-annelated ortho-naphthoquinones and a short synthesis of β-lapachone. *Tetrahedron Lett*. 1993;34: 2437–2440.

[33] Yoshida K, Hayashi A, Mamura T. Jpn Kokai Tokkyo Koho Patent JP 2008195749 A. 2008.

[34] Kurokawa S. The Reaction of Cadalene and Eudalene with Sulfur. *Bull Chem Soc Jpn*. 1970;43:1454–1459.

[35] Konoshima T, Kozuka M, Koyama J, Okatani T, Tagahara K, Tokuda H. Studies on inhibitors of skin tumor promotion, VI. Inhibitory effects of quinones on Epstein-Barr virus activation. *J Nat Prod*. 1989;52:987–995.

[36] Gomez-Monterrey I, Campiglia P, Aquino C, et al. Design, synthesis, and cytotoxic evaluation of acyl derivatives of 3-aminonaphtho[2,3-b]thiophene-4,9-dione, a quinone-based system. *J Med Chem*. 2011;54:4077–4091. https://doi.org/10.1021/jm200094h.

[37] Theodossiou TA, Ali M, Grigalavicius M, et al. Simultaneous defeat of MCF7 and MDA-MB-231 resistances by a hypericin PDT-tamoxifen hybrid therapy. *npj Breast Cancer*. 2019;5:13. https://doi.org/10.1038/s41523-019-0108-8108 [pii].

[38] Thompson EW, Reich R, Shima TB, et al. Differential regulation of growth and invasiveness of MCF-7 breast cancer cells by antiestrogens. *Cancer Res*. 1988;48: 6764–6768.

[39] Cirone M, Gilardini Montani MS, Granato M, Garufi A, Faggioni A, D'Orazi G. Autophagy manipulation as a strategy for efficient anticancer therapies: possible consequences. J Exp Clin Cancer Res 2019;38:262. 10.1186/s13046-019-1275-z10.1186/s13046-019-1275-z [pii].

[40] Ricci MS, Zong WX. Chemotherapeutic approaches for targeting cell death pathways. Oncologist 2006;11:342-57. 11/4/342 [pii]10.1634/theoncologist.11-4-342.

[41] Sui X, Chen R, Wang Z, et al. Autophagy and chemotherapy resistance: a promising therapeutic target for cancer treatment. Cell Death Dis 2013;4:e838. cddis2013350 [pii].

[42] Sun WL, Lan D, Gan TQ, Cai ZW. Autophagy facilitates multidrug resistance development through inhibition of apoptosis in breast cancer cells. *Neoplasma*. 2015;62:199–208. https://doi.org/10.4149/neo_2015_025.

[43] Amani N, Shaki F, Shokrzadeh M. Contribution of Autophagy in Acquired Drug Resistance of Human Breast Cancer Cells MCF7 to Doxorubicin. *Appl In Vitro Toxicol*. 2019;5:173–179.

[44] Han Y, Fan S, Qin T, et al. Role of autophagy in breast cancer and breast cancer stem cells (Review). *Int J Oncol*. Apr 2018;52:1057–1070. https://doi.org/10.3892/ijo.2018.4270.

[45] Qiu W, Su M, Xie F, et al. Tetrandrine blocks autophagic flux and induces apoptosis via energetic impairment in cancer cells. Cell Death Dis 2014;5:e1123. cddis201484 [pii]10.1038/cddis.2014.84.

[46] Zheng L, Zhang Y, Liu G, et al. Tanshinone I regulates autophagic signaling via the activation of AMP-activated protein kinase in cancer cells. *Anticancer Drugs*. Jul 2020;31:601–608. https://doi.org/10.1097/CAD.0000000000000908.

[47] Fu L, Han B, Zhou Y, et al. The Anticancer Properties of Tanshinones and the Pharmacological Effects of Their Active Ingredients. *Front Pharmacol*. 2020;11:193. https://doi.org/10.3389/fphar.2020.00193.

[48] Jian S, Chen L, Minxue L, et al. Tanshinone I induces apoptosis and protective autophagy in human glioblastoma cells via a reactive oxygen speciesdependent pathway. *Int J Mol Med*. Apr 2020;45:983–992. https://doi.org/10.3892/ijmm.2020.4499.

[49] Li C, Han X, Zhang H, Wu J, Li B. The interplay between autophagy and apoptosis induced by tanshinone IIA in prostate cancer cells. *Tumour Biol*. Jun 2016;37: 7667–7674. https://doi.org/10.1007/s13277-015-4602-910.1007/s13277-015-4602-9 [pii].

[50] Dai Y, Grant S. BCL2L11/Bim as a dual-agent regulating autophagy and apoptosis in drug resistance. *Autophagy*. 2015;11:416–418. https://doi.org/10.1080/15548627.2014.998892.

[51] Lindqvist LM, Heinlein M, Huang DC, Vaux DL. Prosurvival Bcl-2 family members affect autophagy only indirectly, by inhibiting Bax and Bak. Proc Natl Acad Sci USA 2014;111:8512-7. 1406425111 [pii]10.1073/pnas.1406425111.

[52] Luo S, Rubinsztein DC. BCL2L11/BIM: a novel molecular link between autophagy and apoptosis. Autophagy 2012;9:104-5. 22399 [pii]10.4161/auto.22399.

[53] Marquez RT, Xu L. Bcl-2: Beclin 1 complex: multiple, mechanisms regulating autophagy/apoptosis toggle switch. *Am J Cancer Res*. 2012;2:214–221.

[54] Menon MB, Dhamija S. Beclin 1 Phosphorylation - at the Center of Autophagy Regulation. *Front Cell Dev Biol*. 2018;6:137. https://doi.org/10.3389/fcell.2018.00137.

[55] Dikic I, Elazar Z. Mechanism and medical implications of mammalian autophagy. *Nat Rev Mol Cell Biol*. Jun 2018;19:349–364. https://doi.org/10.1038/s41580-018-0003-410.1038/s41580-018-0003-4 [pii].

[56] Farre JC, Subramani S. Mechanistic insights into selective autophagy pathways: lessons from yeast. Nat Rev Mol Cell Biol 2016;17:537-52. nrm.2016.74 [pii] 10.1038/nrm.2016.74.

[57] Bhattacharjee S, Bose P, Patel K, et al. Transcriptional and epigenetic modulation of autophagy promotes EBV oncoprotein EBNA3C induced B-cell survival. Cell Death Dis 2018;9:605. 10.1038/s41419-018-0668-910.1038/s41419-018-0668-9 [pii].

[58] Gain C, Malik S, Bhattacharjee S, et al. Proteasomal inhibition triggers viral oncoprotein degradation via autophagy-lysosomal pathway. *PLoS Pathog*. Feb 2020;16. https://doi.org/10.1371/journal.ppat.1008105PPATHOGENS-D-19-01717 [pii].

[59] Fullgrabe J, Ghislat G, Cho DH, Rubinsztein DC. Transcriptional regulation of mammalian autophagy at a glance. J Cell Sci. 2016;129:3059-66. jcs.188920 [pii] 10.1242/jcs.188920.

[60] Di Malta C, Cinque L, Settembre C. Transcriptional Regulation of Autophagy: Mechanisms and Diseases. *Front Cell Dev Biol*. 2019;7:114. https://doi.org/10.3389/fcell.2019.00114.

[61] Avril T, Vauleon E, Chevet E. Endoplasmic reticulum stress signaling and chemotherapy resistance in solid cancers. Oncogenesis 2017;6:e373. oncsis201772 [pii]10.1038/oncsis.2017.72.

[62] Madden E, Logue SE, Healy SJ, Manie S, Samali A. The role of the unfolded protein response in cancer progression: From oncogenesis to chemoresistance. *Biol Cell*. Jan 2019;111:1–17. https://doi.org/10.1111/boc.201800050.

[63] Hetz C, Zhang K, Kaufman RJ. Mechanisms, regulation and functions of the unfolded protein response. *Nat Rev Mol Cell Biol*. Aug 2020;21:421–438. https://doi.org/10.1038/s41580-020-0250-z10.1038/s41580-020-0250-z [pii].

[64] Senft D, Ronai ZA. UPR, autophagy, and mitochondria crosstalk underlies the ER stress response. Trends Biochem Sci 2015;40:141-8. S0968-0004(15)00003-1 [pii] 10.1016/j.tibs.2015.01.002.

[65] Fribley A, Zhang K, Kaufman RJ. Regulation of apoptosis by the unfolded protein response. *Methods Mol Biol*. 2009;559:191–204. https://doi.org/10.1007/978-1-60327-017-5_14.

[66] Rzymski T, Milani M, Pike L, et al. Regulation of autophagy by ATF4 in response to severe hypoxia. Oncogene 2010;29:4424-35. onc2010191 [pii]10.1038/onc.2010.191.

[67] B'Chir W, Maurin AC, Carraro V, et al. The eIF2alpha/ATF4 pathway is essential for stress-induced autophagy gene expression. Nucleic Acids Res 2013;41:7683-99. gkt563 [pii]10.1093/nar/gkt563.
[68] B'Chir W, Chaveroux C, Carraro V, et al. Dual role for CHOP in the crosstalk between autophagy and apoptosis to determine cell fate in response to amino acid deprivation. Cell Signal 2014;26:1385-91. S0898-6568(14)00102-8 [pii]10.1016/j.cellsig.2014.03.009.
[69] Lei Y, Wang S, Ren B, et al. CHOP favors endoplasmic reticulum stress-induced apoptosis in hepatocellular carcinoma cells via inhibition of autophagy. *PLoS ONE*. 2017;12. https://doi.org/10.1371/journal.pone.0183680PONE-D-16-32438 [pii].
[70] Novoa I, Zeng H, Harding HP, Ron D. Feedback inhibition of the unfolded protein response by GADD34-mediated dephosphorylation of eIF2alpha. *J Cell Biol*. 2001;153:1011–1022. https://doi.org/10.1083/jcb.153.5.1011.
[71] Gambardella G, Staiano L, Moretti MN, et al. GADD34 is a modulator of autophagy during starvation. Sci Adv 2020;6. 6/39/eabb0205 [pii]10.1126/sciadv.abb0205.
[72] Mauthe M, Orhon I, Rocchi C, et al. Chloroquine inhibits autophagic flux by decreasing autophagosome-lysosome fusion. *Autophagy*. 2018;14:1435–1455. https://doi.org/10.1080/15548627.2018.1474314.
[73] Galloway WR, Isidro-Llobet A, Spring DR. Diversity-oriented synthesis as a tool for the discovery of novel biologically active small molecules. Nat Commun 2010;1:80. ncomms1081 [pii]10.1038/ncomms1081.